Preprint typeset in JHEP style - PAPER VERSION

Theoretical uncertainties for measurements of α_s from electroweak observables

Hasko Stenzel

II.Physikalisches Institut
Justus-Liebig University of Giessen
Heinrich-Buff Ring 16, D-35392 Giessen, Germany
Hasko.Stenzel@cern.ch

Abstract: One of the most precise measurements of the strong coupling constant $\alpha_s(M_{\rm Z})$ is obtained in the context of global analyses of precision electroweak data. This article reviews the sensitivity of different electroweak observables to α_s and describes the perturbative uncertainties related to missing higher orders. The complete renormalisation scale dependence for the relevant observables is calculated at next-to-next-to-leading order and a new method is presented to determine the corresponding perturbative uncertainty for measurements of α_s based on these observables.

Keywords: e+e- experiments, QCD, Standard Model.

Contents

1. Introduction

High precision measurements of the parameters of the Standard Model (SM) have been performed over the last 15 years in particular at LEP, SLC and TEVATRON. Cross sections, asymmetries, masses and widths of the electroweak (EW) gauge bosons have been determined with a relative accuracy of often better than one per mil. The measurements as a whole over-constrain the SM and allow for an internal consistency check. In a global fit to these data certain unknown parameters like the mass of Higgs boson can be determined, or other quantities not directly measured at LEP like the mass of the top quark can be inferred from the LEP data alone [1]. The sensitivity of the electroweak data to these parameters arise from higher order corrections.

The LEP and SLD experiments have carried out global SM fits to combined data from various experiments and determine five parameters simultaneously: the masses of the Z and Higgs bosons and of the top quark, the hadronic vacuum polarisation $\Delta\alpha^{(5)}_{had}$ and the strong coupling constant $\alpha_s(M_{\mathrm{Z}})$ constitute one often used set of parameters. The

strong coupling constant plays a special role in these fits. It is essentially determined by hadronic observables, for which complete next-to-next-to-leading oder (NNLO) calculations are available. The measurement of α_s benefits from third order $\mathcal{O}(\alpha_s^3)$ perturbative QCD calculation, which is not yet complete for other variables like jet rates, event shapes or fragmentation functions. The theoretical systematic uncertainties related to missing higher orders are expected to be smaller than for NLO-based determinations, even including all-orders resummation used for analyses of event-shape distributions [2].

A detailed analysis of the perturbative uncertainty associated to this kind of measurement of α_s from electroweak observables is the purpose of this article. The renormalisation scale dependence of the theoretical predictions is taken as indicative for the systematic theoretical uncertainty originating from missing higher orders, keeping in mind that the real uncertainty may in fact be different and will be revealed only once the higher orders are actually calculated. Albeit this limitation, the renormalisation scale variation is commonly used in other processes and for other variables as well and may therefore at least be used for a relative comparison of different measurements.

Other methods have been proposed in the past to estimate the uncertainty for EW observables. Instead of a scale variation certain classes of higher oder terms where calculated [3] in order to improve the convergence of the perturbation series by minimising renormalon effects, and the difference with respect to the standard NNLO result was taken as uncertainty. This procedure leads to a very small estimate of ± 0.0005 for the uncertainty of $\alpha_s M_{\mathrm{Z}}$, which should be taken with care given that only a subset of the higher order terms have been calculated.

The scale variation method was investigated in [4], where a parameterisation [5] of R_Z, the ratio of hadronic to leptonic width of the Z boson was used to derive an uncertainty of $+0.0028\ -0.0005$ for α_s. However, the parameterisation embodies only the the scale dependence of the massless NNLO part of the calculation but neglects the also scale dependent massive quark and mixed EW$\otimes$QCD corrections.

The objective of this paper is the complete evaluation of the renormalisation scale dependence for all relevant observables and an analysis of the contribution from different classes of higher order correction to the systematic uncertainty defined by a scale variation.

The experimental systematic uncertainties for α_s are studied in detail by the LEP experiments as well as the correlation between α_s and the other EW observables. Taking the leptonic cross section at the Z pole as observable from which α_s is determined, a variation of the Higgs mass in the range from 100 to 1000 GeV entails a change in α_s of about 0.0022, which has to be compared to an experimental uncertainty of ± 0.0030.

This paper is organised as follows. In Section 2 the EW observables are briefly presented, in Section 3 the theoretical predictions for the widths, the effective couplings and the final state QCD corrections incorporated in the radiator functions are discussed. In Section 4 the theoretical uncertainties of the observables arising from the renormalisation scale variation are evaluated. The scale dependence is used in Section 5 to assess the perturbative uncertainty for measurements of α_s extracted from global fits, supplemented by an experimental cross-check using test data for the EW observables. The conclusion and summary are given in Section 6.

2. Electroweak observables

The sensitivity of certain electroweak observables to α_s arises mainly through pure QCD corrections $\mathcal{O}(\alpha_s^3)$ to the decay widths of the Z boson into hadronic final states. In addition, mixed QCD⊗EW corrections $\mathcal{O}(\alpha\alpha_s)$ to the electroweak couplings give rise to a dependence of both hadronic and leptonic observables on α_s. Numerically the former corrections amount to about three percent, while the mixed corrections, being suppressed by a factor of α, are below one per mil. In practice only observables containing the hadronic or total widths significantly contribute to the determination of α_s

$$\Gamma_h = \sum_q \Gamma_q \ , \ \ \Gamma_q = \Gamma(Z \to q\bar{q}) \ , \ \ \Gamma_Z = \Gamma_h + \Gamma_l + \Gamma_\nu \ . \tag{2.1}$$

Beyond the width itself the R ratio

$$R_Z = \frac{\Gamma_h}{\Gamma_l} \ , \tag{2.2}$$

is of interest as the mixed corrections to the couplings cancel to a large extent in the ratio. For measurements of α_s the most important observables are the leptonic and hadronic pole cross sections

$$\sigma_h^0 = 12\pi \frac{\Gamma_e \Gamma_h}{M_Z^2 \Gamma_Z^2} \ , \ \ \sigma_l^0 = 12\pi \frac{\Gamma_e \Gamma_l}{M_Z^2 \Gamma_Z^2} \ . \tag{2.3}$$

In particular σ_l^0 exhibits a good sensitivity to α_s which allows for a precise measurement of α_s from this observable alone [1]. As the leptonic pole cross section $\sigma_l^0 = \sigma_h^0/R_Z$ is not independent of the other variables, it is not included in the global analyses. Realistic observables are Γ_Z, R_Z and σ_h^0 in the sense that they are independent observables with a substantial sensitivity to α_s.

The calculations presented in this paper are carried out throughout with the electroweak library ZFITTER version 6.36 [6]. If not stated otherwise, the following numerical input values are used:

$$\begin{aligned} M_Z &= 91.1875 \text{ GeV} \\ m_t &= 175 \text{ GeV} \\ M_H &= 150 \text{ GeV} \\ \Delta\alpha_{had}^{(5)}(M_Z^2) &= 0.02761 \\ 1/\alpha(0) &= 137.0359895 \\ \alpha_s(M_Z) &= 0.1185 \end{aligned} \tag{2.4}$$

3. Partial widths

The dependence on α_s and on the renormalisation scale of the relevant EW observables through the widths are given in the following sections.

3.1 Dependence of the widths on α_s

The partial width of the Z decay to a pair of fermions can be cast into two different expressions for leptons and quarks in order to incorporate the different types of radiative corrections. The width for lepton pairs $l = e, \mu, \tau$ is given by:

$$\Gamma_l = \Gamma_0 |\rho_Z^l| \sqrt{1 - \frac{4m_l^2}{M_Z^2}} \left(1 + \frac{3}{4}\frac{\alpha(M_Z^2)}{\pi} Q_l^2\right) \times \left[\left(1 + \frac{2m_l^2}{M_Z^2}\right)(1 + |g_Z^l|^2) - \frac{6m_l^2}{M_Z^2}\right] , \tag{3.1}$$

while for quark pairs $q = u, d, s, c, b$ another expression is used:

$$\Gamma_q = \Gamma_0 \, N_C \, |\rho_Z^q| \Big[|g_Z^q|^2 \, R_V^q(M_Z^2) + R_A^q(M_Z^2) \Big] + \Delta_{\text{EW/QCD}} \, . \tag{3.2}$$

The basic width Γ_0 is the given by

$$\Gamma_0 = \frac{G_\mu M_Z^3}{24\sqrt{2}\,\pi} = 82.945(7)\,\text{MeV} \, , \quad N_C = 3 \, , \tag{3.3}$$

and N_C is a QCD colour factor. In the case of leptons mass effect terms $\propto \frac{m_l^2}{M_Z^2}$ are explicitly taken into account in Eq. 3.1, for quarks these effects are embodied in the radiator functions R_V^q and R_A^q, which also account for QCD and QED radiative corrections. The core of the sensitivity of the widths and related EW observables to α_s stems from the dependence of the radiator functions on α_s, and their renormalisation scale dependence dominates the theoretical uncertainty for a measurement of α_s. The dependence of the widths and derived observables is depicted in Fig. 1, where the change of theses quantities normalised to their value at $\alpha_s(M_\text{Z}) = 0.1185$ is shown. Since the leading term of the QCD correction is $1 + \alpha_s/\pi$, the dependence of the widths on α_s is basically linear, as higher order terms are suppressed by powers of α_s/π.

For the leptonic widths a very small change below 0.1 per mil is observed, induced by two-loop corrections to the effective EW couplings and to the vacuum polarisation contribution to $\alpha(s)$. The hadronic widths exhibit a stronger and opposite dependence resulting in a relative change between 4 and 6 per mil over the range of α_s between 0.11 and 0.13, this dependence is induced by the radiator functions. Among the hadronic widths there are clear differences between up- and down-type quarks, the d- and the s-quark dependences are identical. Furthermore, finite mass quark effects entail small differences between the u- and the c-quark, more visible between the d-quark and the b-quark. The b-quark behaviour is accidentally very close, but not identical to the sum over all flavours.

The dependence of the EW observables on α_s shown in Fig. 1 is, as for the widths, almost linear and the relative change is between 2 and 8 per mil in the considered range. The observable with the strongest dependence is σ_l^0, where the radiator functions enter quadratically in the denominator.

For quarks additional non-factorisable EW⊗QCD corrections $\Delta_{\text{EW/QCD}}$ for the widths are not part of the radiator functions. These corrections are numerically very small (less

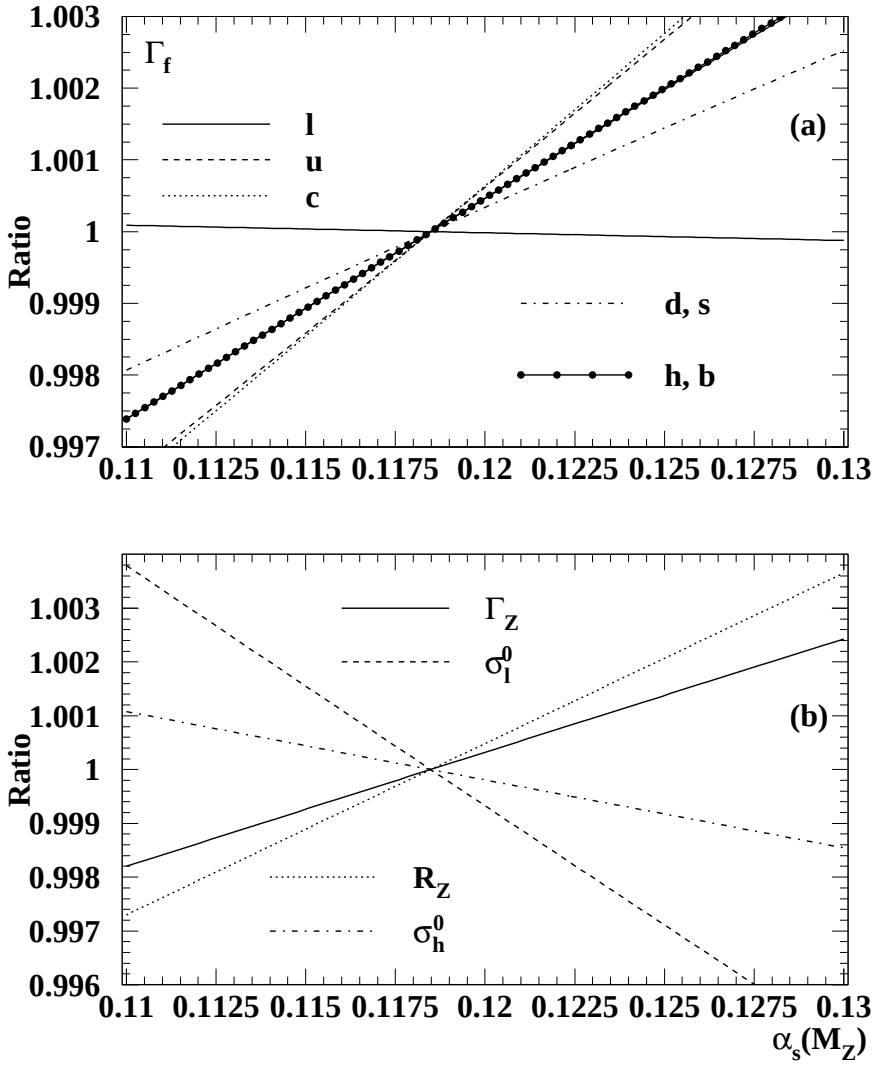

Figure 1: Dependence of the widths (a) and the EW observables (b) on $\alpha_s(M_Z)$. Shown is the normalised ratio of the observable to its reference value at $\alpha_s(M_Z) = 0.1185$. The other SM parameters are kept fixed to their nominal values.

than one per mil) and are taken as fixed numbers from [7, 8]

$$\begin{aligned} \Delta_{\rm EW/QCD} &= -0.113 \text{ MeV} \quad \text{u-, c-quarks} \\ &= -0.160 \text{ MeV} \quad \text{d-, s-quarks} \\ &= -0.040 \text{ MeV} \quad \text{b-quarks} \end{aligned} \tag{3.4}$$

The complex-valued variable ρ_Z^f in Eqs. 3.1, 3.2 measures the overall strength of the neutral current interaction in the $f\bar{f}$ channel and the effective coupling g_Z^f can be expressed in terms

of the ratio of effective vector and axial-vector couplings

$$g_Z^f = \frac{v_f}{a_f} = 1 - 4|Q_f|(\kappa_Z^f s_W^2 + I_f^2) \; , \tag{3.5}$$

where κ_Z^f defines an effective mixing angle for flavour f with $s_W = \sin^2\theta_W$ given by

$$s_W^2 = 1 - c_W^2 \; , \;\; c_W^2 = \frac{M_W^2}{M_Z^2} \; . \tag{3.6}$$

The weak isospin $I_f^{(3)}$ is $\pm 1/2$, the electric charge Q_f is $+\frac{2}{3}/-\frac{1}{3}$ for up-/down-type quarks and the $\mathcal{O}(\alpha^2)$ term I_f^2 originating from $\gamma\gamma$ and $Z\gamma$ polaristion operators is given by

$$I_f^2 = \alpha^2(s)\frac{35}{18}\left[1 - \frac{8}{3}\mathrm{Re}(\kappa_Z^f)s_W^2\right] \; . \tag{3.7}$$

The effective couplings of the Z decay κ_Z^f and ρ_Z^f incorporate radiative electroweak corrections up to two loops and their full expressions are given in [6]. The factorisable EW⊗QCD corrections $\mathcal{O}(\alpha\alpha_s)$ shall be studied here, as they induce the α_s dependence to the effective couplings.

The running QED coupling denoted by $\alpha(s)$ is given by:

$$\alpha(s) = \frac{\alpha(0)}{1 - \Delta\alpha_{had}^{(5)}(s) - \Delta\alpha_{lep}(s) - \Delta\alpha^t(s) - \Delta\alpha^{\alpha\alpha_s}(s)} \; . \tag{3.8}$$

The main contribution to the running coupling stems from the hadronic and leptonic vacuum polarisation. The leptonic part has been calculated at third order [9]

$$\Delta\alpha_{lep}(M_Z^2) = 0.03149767 \; , \tag{3.9}$$

with negligible uncertainties. The hadronic contribution of the five light flavours is related via the dispersion relation to R_γ (equivalent to R_Z in the continuum) from which it can be extracted [10]

$$\Delta\alpha_{had}^{(5)}(M_Z^2) = 0.02761 \pm 0.0036 \; . \tag{3.10}$$

The contribution from the top quark is small but depends on the top quark mass, for $m_t = 175$ GeV

$$\Delta\alpha^t(M_Z^2) = -5.776\ 10^{-5} \; . \tag{3.11}$$

An explicit dependence on α_s appears in the $\mathcal{O}(\alpha\alpha_s)$ correction to $\alpha(s)$ representing gluonic insertions in $t\bar{t}$ loops [11]. Of course the gluon exchange also occurs in light-quark loops and is accounted for in the experimental determination of $\Delta\alpha_{had}^{(5)}$. The correction for the top quark reads

$$\Delta\alpha^t(M_Z^2) = -\frac{\alpha\alpha_s}{\pi^2}\frac{4}{9}\left(\mathrm{Re}\left(\frac{V_1(r_Z)}{r_Z}\right) - 4\zeta(3) + \frac{5}{6}\right) \; , \;\; r_Z = \frac{M_Z^2 + i\epsilon}{4m_t^2} \; , \;\; \zeta(3) = 1.2020569 \; , \tag{3.12}$$

where the expression for $V_1(r)$ is given in [11]. The numerical value is

$$\Delta\alpha^{\alpha\alpha_s}(s) = -1.02\ 10^{-5} \; . \tag{3.13}$$

The dependence of $\alpha(s)$ on α_s is very weak, its relative change is about 10^{-6} for a variation of $\alpha_s(M_Z)$ between 0.11 and 0.13.

3.2 Effective electroweak couplings

The effective electroweak couplings ρ_Z^f and κ_Z^f contain various self-energy terms, calculated for the EW part at NLO with two-loop corrections and at $\mathcal{O}(\alpha\alpha_s)$ for the mixed EW⊗QCD corrections, including the terms leading in m_t of the $\mathcal{O}(\alpha\alpha_s^2)$ contribution. The expressions for EW part are given in [6], here only the terms relevant for the α_s dependence are summarised. In a convenient decomposition ρ_Z^f and κ_Z^f are split into leading and remainder contributions, each being gauge invariant separately. The dominant leading term is resummed to all orders in perturbation theory and the sub-leading remainder is calculated in fixed-order theory. The couplings ρ_Z^f and κ_Z^f can be expanded in the following combination of leading and remainder terms:

$$\rho_Z^f = \frac{1 + f_\alpha \left(\rho_{rem}^{f,G} + \rho_{rem}^{f,G\alpha_s}\right) + \rho_{rem}^{f,G^2}}{1 + (\hat{\rho}^G + \hat{\rho}^{G\alpha_s})\left(1 - \Delta r_{rem}^G - \Delta r_{rem}^{G\alpha_s}\right)} , \tag{3.14}$$

$$\begin{aligned}\kappa_Z^f = &\left[1 + f_\alpha \left(\kappa_{rem}^{f,G} + \kappa_{rem}^{f,G\alpha_s}\right) + \kappa_{rem}^{f,G^2}\right] \\ &\times \left[1 - \frac{c_W^2}{s_W^2}\left(\hat{\rho}^G + \hat{\rho}^{G\alpha_s}\right)\left(1 - \Delta r_{rem}^G - \Delta r_{rem}^{G\alpha_s}\right)\right] .\end{aligned} \tag{3.15}$$

The transformation factor f_α accounts for the conversion of couplings $\alpha \to G_\mu$ [12]

$$f_\alpha = \frac{\sqrt{2} G_\mu M_{\mathrm{Z}} s_W^2 c_W^2}{\pi\alpha} . \tag{3.16}$$

The three-loop QCD correction to the ρ parameter arising from top-quark loops is given by [13]

$$\begin{aligned}\hat{\rho}^{G\alpha_s} &= 3x_t \left(c_{t1}\frac{\alpha_s(m_t)}{\pi} + c_{t2}\left(\frac{\alpha_s(m_t)}{\pi}\right)^2\right) , \\ x_t &= \frac{G_\mu m_t^2}{8\pi^2\sqrt{2}} , \;\; c_{t1} = -2.86 , \;\; c_{t2} = -18.18 ,\end{aligned} \tag{3.17}$$

which also includes corrections to the term leading in $G_\mu m_t^2 \alpha_s^2$ derived in [14]. This is the dominant QCD correction to ρ_Z^f and κ_Z^f and its renormalisation scale dependence determine the perturbative uncertainty for ρ_Z^f and κ_Z^f derived in Section 4.

The expansions of ρ_Z^f and κ_Z^f have also the remainders of the renormalisation parameter Δr [6] in common, the component containing the QCD corrections is given by

$$\Delta r_{rem}^{G\alpha_s} = tb - tbl + 2cl , \tag{3.18}$$

$$tb = \frac{\alpha\alpha_s(m_t)}{\pi^2} dr_{rem}\left(M_{\mathrm{Z}}, M_{\mathrm{W}}, m_t^2\right) , \tag{3.19}$$

$$tbl = \frac{\alpha\alpha_s(m_t)}{4\pi^2}\frac{m_t^2}{M_{\mathrm{W}}^2}\frac{M_{\mathrm{Z}}^2}{M_{\mathrm{Z}}^2 - M_{\mathrm{W}}^2}\left(\frac{1}{2} + \frac{\pi^2}{6}\right) , \tag{3.20}$$

$$cl = -\frac{\alpha\alpha_s(M_Z)}{4\pi^2}\frac{M_{\mathrm{Z}}^2 M_{\mathrm{W}}^2}{(M_{\mathrm{Z}}^2 - M_{\mathrm{W}}^2)^2}\log\left(\frac{M_{\mathrm{W}}^2}{M_{\mathrm{Z}}^2}\right)$$

$$\times \left[1 + c_{l1}\frac{\alpha_s(M_Z)}{\pi} + c_{l2}\left(\frac{\alpha_s(M_Z)}{\pi}\right)^2\right] , \tag{3.21}$$

$$c_{l1} = 1.409 , \quad c_{l2} = -12.805 . \tag{3.22}$$

The QCD correction for the flavour-dependent remainder of ρ_Z^f is

$$\rho_{rem}^{f,G\alpha_s} = \rho^{QCD} + tbl , \tag{3.23}$$

$$\rho^{QCD} = \frac{\alpha\alpha_s(m_t)}{\pi^2} d\rho_{rem}\left(M_{\rm Z}, M_{\rm W}, m_t^2\right) + \frac{\alpha\alpha_s(M_Z)}{\pi^2}\frac{V_T^2(t) + V_T^2(b) + 2}{8 s_W^2 c_W^2} , \tag{3.24}$$

$$V_T(q) = 1 - 4Q_q s_W^2 \tag{3.25}$$

The expression for κ_Z^f contains another QCD correction for the remainder

$$\kappa_{rem}^{f,G\alpha_s} = \kappa^{QCD} + \frac{M_W^2}{M_Z^2 - M_W^2} tbl - 3 x_t c_{a2}\left(\frac{\alpha_s(m_t)}{\pi}\right)^2 , \tag{3.26}$$

$$c_{a2} = 0.644 , \tag{3.27}$$

$$\kappa^{QCD} = \frac{\alpha\alpha_s(m_t)}{\pi^2} d\kappa_{rem}\left(M_{\rm Z}, M_{\rm W}, m_t^2\right) \tag{3.28}$$

$$+\frac{\alpha\alpha_s(M_Z)}{\pi^2}\frac{c_W^2}{2 s_W^4}\log c_W^2 \tag{3.29}$$

The remainder functions $dr_{rem}, d\rho_{rem}$ and $d\kappa_{rem}$ describing the $\mathcal{O}(\alpha\alpha_s)$ contribution to the bosonic self-energies have been derived analytically in [11].

In the case of b-quarks two additional one-loop vertex diagrams, absent for light quarks, are generated by the large mass splitting between the t- and the b-quark and contribute to the widths Γ_b [15]. These corrections entail a modification of the $Zb\bar{b}$ decay amplitude form factor [6], which in turn affects the effective couplings. If ρ' and κ' denote the modified couplings given in [6], then the corrected couplings for the b quark are obtained by

$$\rho_Z^b = \rho'\left(1 + \tau_b\right)^2 , \tag{3.30}$$

$$\kappa_Z^b = \frac{\kappa'}{1 + \tau_b} , \tag{3.31}$$

$$\tau_b = -2 x_t\left(1 - \frac{\pi}{3}\alpha_s(m_t) + x_t \tau_2 \frac{m_t^2}{M_H^2}\right) , \tag{3.32}$$

where the term in $\alpha_s(m_t)$ was obtained by [16] and the expression for τ_2 can be found in [17].

The dependence of the couplings on α_s is shown in Fig.2 for the absolute value of ρ_Z^f and the squared module of g_Z^f, these are the relevant terms for the widths according to Eqs. 3.1, 3.2. The dependence of ρ_Z^f on α_s is weak, the relative change in the considered range is below $2 \cdot 10^{-4}$. All quark flavours and the leptons exhibit practically the same α_s dependence, except the b-quark for which it is even weaker and opposite.

The representation of the relative change as ratio is inadequate for $|g_Z^f|^2$ since its absolute value is rather small, e.g. for leptons $|g_Z^l|^2 = 0.00555$ and $|\rho_Z^l| = 1.00517$ at

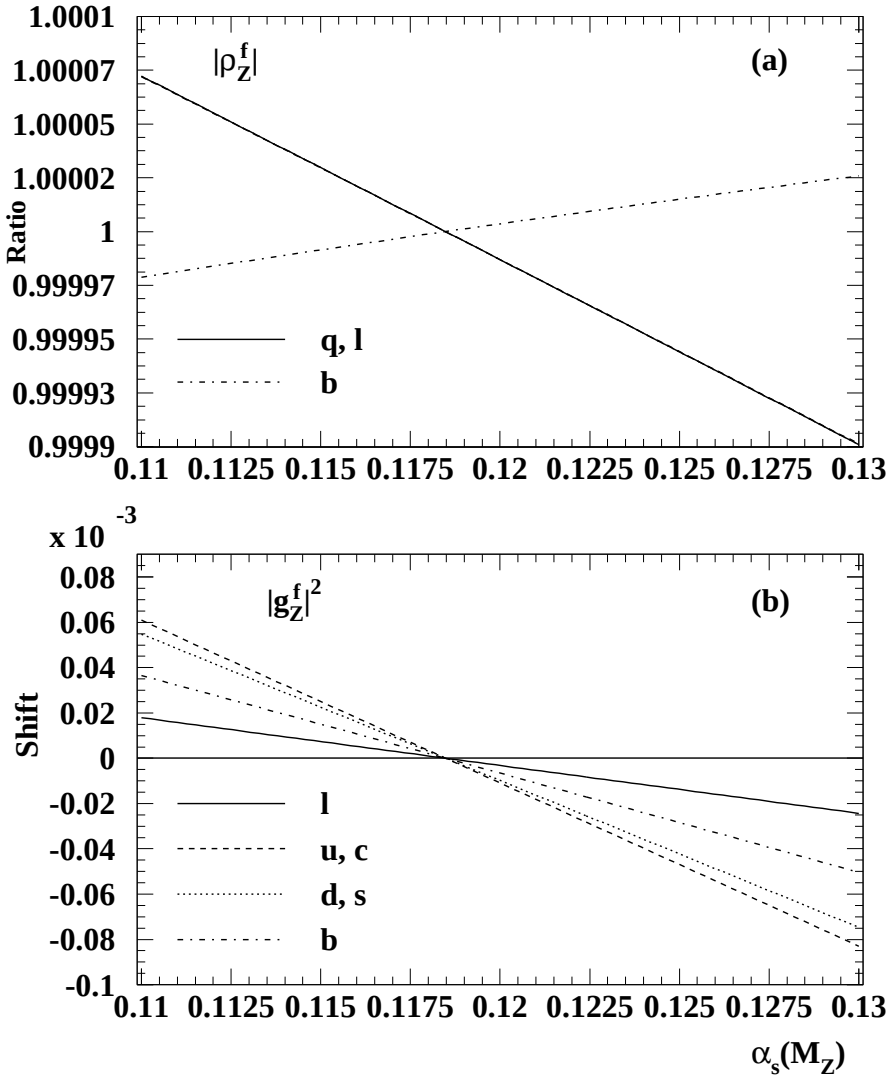

Figure 2: Dependence of the $|\rho_Z^f|$ (a) and $|g_Z^f|^2$ (b) on $\alpha_s(M_\mathrm{Z})$. For $|\rho_Z^f|$ the normalised ratio and for $|g_Z^f|^2$ the shift of the coupling to its reference value at $\alpha_s(M_\mathrm{Z}) = 0.1185$ is shown.

$\alpha_s(M_\mathrm{Z}) = 0.1185$. Instead the shift defined by $|g_Z^f|^2(\alpha_s) - |g_Z^f|^2(\alpha_s = 0.1185)$ is a better indicator for the dependence on α_s. The absolute change of $|g_Z^f|^2$ is between $1.4 \cdot 10^{-4}$ for up-type quarks and $0.4 \cdot 10^{-4}$ for leptons. This translates into a relative change much larger for leptons than for quarks, given the small size of $|g_Z^l|^2$ for the leptons.

The observed α_s dependence of the leptonic widths shown in Fig. 1 is dominated by dependence of ρ_Z^f on α_s. In the case of quarks, however, the couplings contribution to the α_s dependence of the widths is sub-leading, the main properties are determined by the QCD final state corrections in the radiator functions.

3.3 Radiator functions

Final state QCD and QED vector and axial vector corrections to the quarkonic widths Eq. 3.2 are embodied in the radiator functions

$$
\begin{aligned}
R_V^q(s) = 1 &+ \frac{3}{4}Q_q^2\frac{\alpha(s)}{\pi} + \frac{\alpha_s(s)}{\pi} - \frac{1}{4}Q_q^2\frac{\alpha(s)}{\pi}\frac{\alpha_s(s)}{\pi} \\
&+ \left[C_{02} + C_2^t\left(\frac{s}{m_t^2}\right)\right]\left(\frac{\alpha_s(s)}{\pi}\right)^2 + C_{03}\left(\frac{\alpha_s(s)}{\pi}\right)^3 \\
&+ \frac{m_c^2(s)+m_b^2(s)}{s}C_{23}\left(\frac{\alpha_s(s)}{\pi}\right)^3 \\
&+ \frac{m_q^2(s)}{s}\left[C_{21}^V\frac{\alpha_s(s)}{\pi} + C_{22}^V\left(\frac{\alpha_s(s)}{\pi}\right)^2 + C_{23}^V\left(\frac{\alpha_s(s)}{\pi}\right)^3\right] \\
&+ \frac{m_c^4(s)}{s^2}\left[C_{42} - \ln\frac{m_c^2(s)}{s}\right]\left(\frac{\alpha_s(s)}{\pi}\right)^2 + \frac{m_b^4(s)}{s^2}\left[C_{42} - \ln\frac{m_b^2(s)}{s}\right]\left(\frac{\alpha_s(s)}{\pi}\right)^2 \\
&+ \frac{m_q^4(s)}{s^2}\left\{C_{41}^V\frac{\alpha_s(s)}{\pi} + \left[C_{42}^V + C_{42}^{V,L}\ln\frac{m_q^2(s)}{s}\right]\left(\frac{\alpha_s(s)}{\pi}\right)^2\right\} \\
&+ 12\frac{m_q'^4(s)}{s^2}\left(\frac{\alpha_s(s)}{\pi}\right)^2 - \frac{m_q^6(s)}{s^3}\left\{8 + \frac{16}{27}\left[155 + 6\ln\frac{m_q^2(s)}{s}\right]\frac{\alpha_s(s)}{\pi}\right\}, \qquad (3.33)
\end{aligned}
$$

$$
\begin{aligned}
R_A^q(s) = 1 &+ \frac{3}{4}Q_q^2\frac{\alpha(s)}{\pi} + \frac{\alpha_s(s)}{\pi} - \frac{1}{4}Q_q^2\frac{\alpha(s)}{\pi}\frac{\alpha_s(s)}{\pi} \\
&+ \left[C_{02} + C_2^t\left(\frac{s}{m_t^2}\right) - \left(2I_q^{(3)}\right)\mathcal{I}^{(2)}\left(\frac{s}{m_t^2}\right)\right]\left(\frac{\alpha_s(s)}{\pi}\right)^2 \\
&+ \left[C_{03} - \left(2I_q^{(3)}\right)\mathcal{I}^{(3)}\left(\frac{s}{m_t^2}\right)\right]\left(\frac{\alpha_s(s)}{\pi}\right)^3 \\
&+ \frac{m_c^2(s)+m_b^2(s)}{s}C_{23}\left(\frac{\alpha_s(s)}{\pi}\right)^3 + \frac{m_q^2(s)}{s}\left[C_{20}^A + C_{21}^A\frac{\alpha_s(s)}{\pi} + C_{22}^A\left(\frac{\alpha_s(s)}{\pi}\right)^2\right. \\
&\left.+ 6\left(3 + \ln\frac{m_t^2}{s}\right)\left(\frac{\alpha_s(s)}{\pi}\right)^2 + C_{23}^A\left(\frac{\alpha_s(s)}{\pi}\right)^3\right] \\
&- 10\frac{m_q^2(s)}{m_t^2}\left[\frac{8}{81} + \frac{1}{54}\ln\frac{m_t^2}{s}\right]\left(\frac{\alpha_s(s)}{\pi}\right)^2 \\
&+ \frac{m_c^4(s)}{s^2}\left[C_{42} - \ln\frac{m_c^2(s)}{s}\right]\left(\frac{\alpha_s(s)}{\pi}\right)^2 + \frac{m_b^4(s)}{s^2}\left[C_{42} - \ln\frac{m_b^2(s)}{s}\right]\left(\frac{\alpha_s(s)}{\pi}\right)^2 \\
&+ \frac{m_q^4(s)}{s^2}\left\{C_{40}^A + C_{41}^A\frac{\alpha_s(s)}{\pi} + \left[C_{42}^A + C_{42}^{A,L}\ln\frac{m_q^2(s)}{s}\right]\left(\frac{\alpha_s(s)}{\pi}\right)^2\right\} \\
&- 12\frac{m_q'^4(s)}{s^2}\left(\frac{\alpha_s(s)}{\pi}\right)^2. \qquad (3.34)
\end{aligned}
$$

Finite mass corrections are retained only for the b- and c-quark, i.e. $m_q = 0$ for q=u,d,s, and the terms $m_q(s)$ represent the running quark masses in the $\overline{\rm MS}$ scheme. The term m_q'

denotes the other quark mass in doublet, it is m_c for q=b and m_b for q=c. The different terms of Eq. 3.33 and Eq. 3.34 and their coefficients can be organised in the following classes of corrections.
Massless non-singlet corrections [18–21]:

$$C_{02} = \frac{365}{24} - 11\,\zeta(3) + \left[-\frac{11}{12} + \frac{2}{3}\,\zeta(3)\right] n_f, \tag{3.35}$$

$$\begin{aligned} C_{03} = {} & \frac{87029}{288} - \frac{121}{8}\,\zeta(2) - \frac{1103}{4}\,\zeta(3) + \frac{275}{6}\,\zeta(5) \\ & + \left[-\frac{7847}{216} + \frac{11}{6}\,\zeta(2) + \frac{262}{9}\,\zeta(3) - \frac{25}{9}\,\zeta(5)\right] n_f \\ & + \left[\frac{151}{162} - \frac{1}{18}\,\zeta(2) - \frac{19}{27}\,\zeta(3)\right] n_f^2, \end{aligned} \tag{3.36}$$

with the number of active flavours n_f.
Quadratic massive corrections [22]:

$$C_{23} = -80 + 60\,\zeta(3) + \left[\frac{32}{9} - \frac{8}{3}\,\zeta(3)\right] n_f, \tag{3.37}$$

$$C_{21}^V = 12, \tag{3.38}$$

$$C_{22}^V = \frac{253}{2} - \frac{13}{3} n_f, \tag{3.39}$$

$$\begin{aligned} C_{23}^V = {} & 2522 - \frac{855}{2}\,\zeta(2) + \frac{310}{3}\,\zeta(3) - \frac{5225}{6}\,\zeta(5) \\ & + \left[-\frac{4942}{27} + 34\,\zeta(2) - \frac{394}{27}\,\zeta(3) + \frac{1045}{27}\,\zeta(5)\right] n_f + \left[\frac{125}{54} - \frac{2}{3}\,\zeta(2)\right] n_f^2, \end{aligned} \tag{3.40}$$

$$C_{20}^A = -6, \tag{3.41}$$

$$C_{21}^A = -22, \tag{3.42}$$

$$C_{22}^A = -\frac{8221}{24} + 57\,\zeta(2) + 117\,\zeta(3) + \left[\frac{151}{12} - 2\,\zeta(2) - 4\,\zeta(3)\right] n_f, \tag{3.43}$$

$$\begin{aligned} C_{23}^A = {} & -\frac{4544045}{864} + 1340\,\zeta(2) + \frac{118915}{36}\,\zeta(3) - 127\,\zeta(5) \\ & + \left[\frac{71621}{162} - \frac{209}{2}\,\zeta(2) - 216\,\zeta(3) + 5\zeta(4) + 55\,\zeta(5)\right] n_f \\ & + \left[-\frac{13171}{1944} + \frac{16}{9}\,\zeta(2) + \frac{26}{9}\,\zeta(3)\right] n_f^2; \end{aligned} \tag{3.44}$$

Quartic massive corrections:

$$C_{42} = \frac{13}{3} - 4\,\zeta(3), \tag{3.45}$$

$$C_{40}^V = -6, \tag{3.46}$$

$$C_{41}^V = -22, \tag{3.47}$$

$$C_{42}^V = -\frac{3029}{12} + 162\,\zeta(2) + 112\,\zeta(3) + \left[\frac{143}{18} - 4\,\zeta(2) - \frac{8}{3}\,\zeta(3)\right] n_f, \tag{3.48}$$

$$C_{42}^{V,L} = -\frac{11}{2} + \frac{1}{3} n_f, \tag{3.49}$$

$$C_{40}^A = 6, \tag{3.50}$$

$$C_{41}^A = 10, \tag{3.51}$$

$$C_{42}^A = \frac{3389}{12} - 162\,\zeta(2) - 220\,\zeta(3) + \left[-\frac{41}{6} + 4\,\zeta(2) + \frac{16}{3}\,\zeta(3)\right] n_f, \tag{3.52}$$

$$C_{42}^{A,L} = \frac{77}{2} - \frac{7}{3} n_f; \tag{3.53}$$

Power suppressed t-quark mass correction:

$$C_2^t(x) = x\left(\frac{44}{675} - \frac{2}{135}\ln x\right); \tag{3.54}$$

Singlet axial corrections:

$$\mathcal{I}^{(2)}(x) = -\frac{37}{12} + \ln x + \frac{7}{81} x + 0.0132 x^2, \tag{3.55}$$

$$\mathcal{I}^{(3)}(x) = -\frac{5075}{216} + \frac{23}{6}\,\zeta(2) + \zeta(3) + \frac{67}{18}\ln x + \frac{23}{12}\ln^2 x. \tag{3.56}$$

Here, the Riemann Zeta function ζ is defined by

$$\zeta(x) = \sum_{n=1}^{\infty} n^{-x} \tag{3.57}$$

with particular values

$$\zeta(2) = 1.6449341\ , \quad \zeta(3) = 1.2020569\ , \quad \zeta(5) = 1.0369278\ . \tag{3.58}$$

The evolution of the radiator functions with α_s is shown in Fig. 3. The vector radiator functions for the different flavours are very similar and can barely be distinguished. Their dependence on α_s is almost linear and they are increasing by 0.6% for a change of α_s from 0.11 to 0.13. The axial-vector radiator function exhibits a prominent flavour dependence. For up-type quarks R_A^q increases by 0.8%, for down-type quarks the change of the axial-vector radiator function is only of 0.4%. The third component of the weak isospin $I_q^{(3)}$,

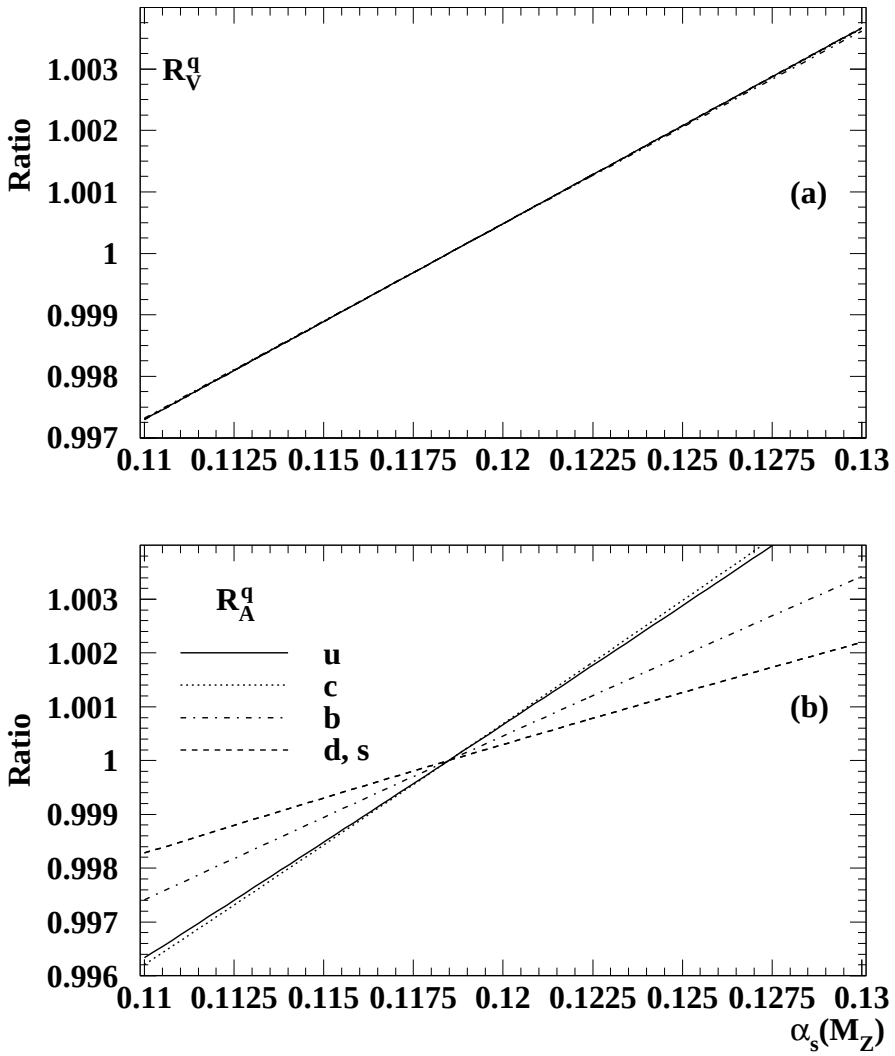

Figure 3: Dependence of the radiator functions R_V^q (a) and R_A^q (b) on $\alpha_s(M_\mathrm{Z})$. The ratio of the radiator function at a given value of $\alpha_s(M_\mathrm{Z})$ and the reference value at $\alpha_s(M_\mathrm{Z}) = 0.1185$ is shown.

present in the singlet axial component of R_A^q, generates the up/down-quark difference. On top of this difference the b-quark mass corrections are important and entail a change of R_A^b of 0.6%.

3.3.1 Running quark masses

The running quark masses $m_q(s)$ in the $\overline{\mathrm{MS}}$ scheme are related to the fixed-valued pole masses M_q. For the c-quark at $s = M_s^2$ and $n_f = 4$ it follows

$$M_c = m_c(M_c^2)\left\{1 + \left[\frac{4}{3} + \ln\frac{M_c^2}{m_c^2(M_c^2)}\right]\frac{\alpha_s(M_c^2)}{\pi}\right.$$

$$+\left[K_c+\left(\frac{173}{24}-\frac{13}{36}n_f\right)\ln\frac{M_c^2}{m_c^2(M_c^2)}+\left(\frac{15}{8}-\frac{1}{12}n_f\right)\ln^2\frac{M_c^2}{m_c^2(M_c^2)}\right.$$
$$\left.+\frac{4}{3}\Xi\left(\frac{m_s(M_c^2)}{m_c(M_c^2)}\right)\right]\left(\frac{\alpha_s(M_c^2)}{\pi}\right)^2\Bigg\}, \tag{3.59}$$

with

$$K_c=\frac{2905}{288}+\frac{1}{3}\left[7+2\ln(2)\right]\zeta(2)-\frac{1}{6}\zeta(3)-\frac{1}{3}\left[\frac{71}{48}+\zeta(2)\right]n_f, \tag{3.60}$$

$$\Xi(x)=\frac{\pi^2}{8}x-0.597x^2+0.23x^3. \tag{3.61}$$

The running mass is evolved according to the renormalisation group equation from the scale of the pole mass M_c^2 to the scale of the process s in a two-step evolution $M_c^2\to M_b^2\to s$:

$$\begin{aligned}m_c(s)=m_c(M_c^2)&\left[\frac{\alpha_s(M_b^2)}{\alpha_s(M_c^2)}\right]^{\gamma_0^{(4)}/\beta_0^{(4)}}\left\{1+C_1(4)\left[\frac{\alpha_s(M_b^2)}{\pi}-\frac{\alpha_s(M_c^2)}{\pi}\right]\right.\\
&\left.+\frac{1}{2}C_1^2(4)\left[\frac{\alpha_s(M_b^2)}{\pi}-\frac{\alpha_s(M_c^2)}{\pi}\right]^2+\frac{1}{2}C_2(4)\left[\left(\frac{\alpha_s(M_b^2)}{\pi}\right)^2-\left(\frac{\alpha_s(M_c^2)}{\pi}\right)^2\right]\right\}\\
&\times\left[\frac{\alpha_s(s)}{\alpha_s(M_b^2)}\right]^{\gamma_0^{(5)}/\beta_0^{(5)}}\left\{1+C_1(5)\left[\frac{\alpha_s(s)}{\pi}-\frac{\alpha_s(M_b^2)}{\pi}\right]\right.\\
&\left.+\frac{1}{2}C_1^2(5)\left[\frac{\alpha_s(s)}{\pi}-\frac{\alpha_s(M_b^2)}{\pi}\right]^2+\frac{1}{2}C_2(5)\left[\left(\frac{\alpha_s(s)}{\pi}\right)^2-\left(\frac{\alpha_s(M_b^2)}{\pi}\right)^2\right]\right\}.\end{aligned} \tag{3.62}$$

For the running b-quark mass the same procedure is applied with a single evolution from M_b^2 to s. The coefficients in Eq. 3.62 are given by:

$$C_1(n_f)=\frac{\gamma_1^{(n_f)}}{\beta_0^{(n_f)}}-\frac{\beta_1^{(n_f)}\gamma_0^{(n_f)}}{\left(\beta_0^{(n_f)}\right)^2}, \tag{3.63}$$

$$C_2(n_f)=\frac{\gamma_2^{(n_f)}}{\beta_0^{(n_f)}}-\frac{\beta_1^{(n_f)}\gamma_1^{(n_f)}}{\left(\beta_0^{(n_f)}\right)^2}-\frac{\beta_2^{(n_f)}\gamma_0^{(n_f)}}{\left(\beta_0^{(n_f)}\right)^2}+\frac{\left(\beta_1^{(n_f)}\right)^2\gamma_0^{(n_f)}}{\left(\beta_0^{(n_f)}\right)^3}. \tag{3.64}$$

The coefficients of the Beta and Gamma functions are:

$$\beta_0^{(n_f)}=\frac{1}{4}\left(11-\frac{2}{3}n_f\right), \tag{3.65}$$

$$\beta_1^{(n_f)}=\frac{1}{16}\left(102-\frac{38}{3}n_f\right), \tag{3.66}$$

$$\beta_2^{(n_f)}=\frac{1}{64}\left(\frac{2857}{2}-\frac{5033}{18}n_f+\frac{325}{54}n_f^2\right), \tag{3.67}$$

$$\gamma_0^{(n_f)} = 1, \tag{3.68}$$

$$\gamma_1^{(n_f)} = \frac{1}{16}\left(\frac{202}{3} - \frac{20}{9}n_f\right), \tag{3.69}$$

$$\gamma_2^{(n_f)} = \frac{1}{64}\left\{1249 - \left[\frac{2216}{27} + \frac{160}{3}\,\zeta(3)\right] n_f - \frac{140}{81}n_f^2\right\}. \tag{3.70}$$

The renormalisation scale dependence of the coupling constant can be parameterised at 3-loop level as function of $\Lambda_{\overline{\rm MS}}^{(nf)}$

$$\alpha_s(\mu) = \frac{\pi}{\beta_0 \ln(\mu^2/\Lambda^2)}\left[1 - \frac{\beta_1}{\beta_0^2}\frac{\ln\left[\ln(\mu^2/\Lambda^2)\right]}{\ln(\mu^2/\Lambda^2)} + \frac{1}{\beta_0^2 \ln^2(\mu^2/\Lambda^2)} \times \right.$$
$$\left. \times \left(\frac{\beta_1^2}{\beta_0^2}\left\{\ln^2\left(\frac{\mu^2}{\Lambda^2}\right) - \ln\left[\ln\left(\frac{\mu^2}{\Lambda^2}\right)\right] - 1\right\} + \frac{\beta_2}{\beta_0}\right)\right]. \tag{3.71}$$

Technically, for a given input value of $\alpha_s(M_{\rm Z})$, Eq. 3.71 is solved numerically for $n_f = 5$ in order to obtain $\Lambda_{\overline{\rm MS}}^{(5)}$. The scale parameters for $n_f = 4$ and $n_f = 3$, $\Lambda_{\overline{\rm MS}}^{(4)}$ and $\Lambda_{\overline{\rm MS}}^{(3)}$, required for the evolution of α_s to the scales of the quark pole masses M_b and M_c, are derived using the matching condition

$$\ln\left(\frac{\Lambda_{\overline{\rm MS}}^{(n_f)}}{\Lambda_{\overline{\rm MS}}^{(n_f-1)}}\right)^2 = \beta_0^{(n_f-1)}\left\{\left(\beta_0^{(n_f)} - \beta_0^{(n_f-1)}\right) L_M + \left(\frac{\beta_1^{(n_f)}}{\beta_0^{(n_f)}} - \frac{\beta_1^{(n_f-1)}}{\beta_0^{(n_f-1)}}\right)\ln L_M \right.$$
$$- \frac{\beta_1^{(n_f-1)}}{\beta_0^{(n_f-1)}}\ln\frac{\beta_0^{(n_f)}}{\beta_0^{(n_f-1)}} + \frac{\beta_1^{(n_f)}}{\left(\beta_0^{(n_f)}\right)^2}\left(\frac{\beta_1^{(n_f)}}{\beta_0^{(n_f)}} - \frac{\beta_1^{(n_f-1)}}{\beta_0^{(n_f-1)}}\right)\frac{\ln L_M}{L_M}$$
$$\left. + \frac{1}{\beta_0^{(n_f)}}\left[\left(\frac{\beta_1^{(n_f)}}{\beta_0^{(n_f)}}\right)^2 - \left(\frac{\beta_1^{(n_f-1)}}{\beta_0^{(n_f-1)}}\right)^2 - \frac{\beta_2^{(n_f)}}{\beta_0^{(n_f)}} + \frac{\beta_2^{(n_f-1)}}{\beta_0^{(n_f-1)}} - \frac{7}{72}\right]\frac{1}{L_M}\right\}, \tag{3.72}$$

with

$$L_M = \ln\frac{M_q^2}{\left(\Lambda_{\overline{\rm MS}}^{(n_f)}\right)^2}\,. \tag{3.73}$$

3.4 Quantifying higher order contributions

The theoretical prediction for the widths and derived EW observables consists of three basic ingredients, each incorporating different classes of higher order contributions: the NNLO massless terms, the quark mass corrections and the mixed EW⊗QCD corrections. For the evaluation of associated perturbative uncertainties it is essential to study the impact and size of the these contributions to the full theory. The sensitivity of widths and realistic observables to the three classes of corrections is illustrated in Table 1, where the relative

Theory	NNLO		NLO	without quark mass corrections	without mixed corrections
Γ_u	300.057	MeV	−0.13	0.00	1.66
$\Gamma_{d,s}$	382.901	MeV	1.28	0.00	1.45
Γ_c	299.994	MeV	−0.18	0.21	1.67
Γ_b	375.807	MeV	1.23	4.13	1.47
Γ_h	1741.66	MeV	0.77	0.93	1.53
Γ_l	83.796	MeV	0.00	0.00	1.19
Γ_Z	2495.08	MeV	0.54	0.65	1.37
σ_h^0	41.4798	nb	−0.31	−0.37	−0.03
σ_l^0	2.0002	nb	−1.08	−1.29	−0.37
R_Z	20.737		0.78	0.93	0.34
	nominal value		relative change [‰]		

Table 1: Nominal values of widths and EW observables and their relative change in per mil observed when certain classes of corrections are omitted. The calculations are carried out for $\alpha_s(M_Z) = 0.1185$.

change of the full prediction with respect to downgraded calculations neglecting certain terms is given. The change from NNLO to NLO for the quarkonic widths is between one per mil for down-type quarks and 0.1 per mil for up-type quarks, this large difference is generated by flavour-dependent contributions to R_A^q and g_Z^q. Neither NNLO nor quark mass corrections have any sizeable impact on the leptonic width, but the mixed EW⊗QCD corrections entail changes of 1.5 per mil to all widths, larger than the final state NNLO corrections. Not surprisingly, the quark mass corrections are as large as 4 per mil for b-quarks but drop to 0.2 per mil for c-quarks. The total width absorbs an average effect induced by the widths and the other realistic observables are in general less sensitive to these corrections cancelling in the ratio of widths. Among the realistic observables σ_h^0 is least and σ_l^0 most sensitive to the higher order corrections, their size ranges between 0.3 and 1.3‰.

4. Theoretical uncertainties for EW observables

The sensitivity of a given electroweak observable to α_s originate on one side from the QCD corrections incorporated in the radiator functions and on the other side from the mixed EW⊗QCD corrections to the effective couplings. A measurement of α_s using EW observables is subject to a systematic uncertainty stemming from missing higher orders in the perturbation series. The yet uncalculated higher orders are inherently difficult to access. A conventional method of estimating the perturbative uncertainty consists of a variation of the renormalisation scale μ. The natural scale of the process is usually taken to be $\sqrt{s}$ in e^+e^- annihilation, and subsequently in the case of Z peak observables μ is set to M_Z. Neither this particular choice for the nominal scale nor the range of variation for μ are unambiguous [2]. Following the convention applied in analyses of e^+e^- event-shape

variables, the perturbative uncertainty is estimated by changing $x_\mu = \mu/\sqrt{s}$ in the range $1/2 \leq x_\mu \leq 2$.

A variation of the renormalisation scale induces a change of the value of $\alpha_s(\mu)$ as given in Eq. 3.71. At NLO and beyond this change is compensated by a modification of the (N)NLO terms, resulting in a residual dependence at (N)NNLO. The details of the scale dependence of the radiator functions is discussed below.

The mixed $\mathcal{O}(\alpha\alpha_s)$ corrections are complete only at leading order in α_s, but the dominant three-loop correction in Eq. 3.17 leading in m_t^2 is included. For these $\mathcal{O}(\alpha\alpha_s^2)$ terms the explicit scale dependence is taken into account.

Given the overall small size of the EW⊗QCD corrections, they do not contribute significantly to the scale dependence of the realistic observables.

4.1 Renormalisation scale dependence

Dimensional regularisation introduces a renormalisation scale μ at which the coupling constant is defined. Thereby, the coefficients in the expansion of $R^q_{V,A}$ acquire an explicit dependence on this scale, which is only at all orders completely compensated by the scale dependence of $\alpha_s(\mu)$. For a NNLO calculation, the residual scale dependence is N^{3}LO. The nominal value of the μ scale is set to the scale of the process $\mu^2 = s$.

The expression for $R^q_{V,A}$ in Eqs. 3.33, 3.34 are valid only for $\mu^2 = s$, for different renormalisation scales terms proportional to powers of $\ln \mu^2/s$ appear. For a generic power series of the type

$$R = \sum_{i=0}^{n} c_n \left(\frac{\alpha_s}{\pi}\right)^n \ , \tag{4.1}$$

the NLO coefficient c_2 becomes a function of μ

$$c_2 \to c_2(\mu) = c_2 + \beta_0 c_1 \ln \frac{\mu^2}{s} \ . \tag{4.2}$$

It is important to note that two quantities depend on the renormalisation scale in Eqs. 3.33 and 3.34: the coupling constant $\alpha_s(\mu)$ (Eq. 3.71) and the running masses $m_q(\mu)$ (Eq. 3.62).

In order to to simplify the formulae for the scale dependence of the radiator functions, it is convenient to re-order Eqs. 3.33 and 3.34 in terms of powers of the running masses:

$$R^q_{V,A}(\mu) = \sum_{f=q,q',c,b} \sum_{i=0}^{3} \frac{m_f^{2i}(\mu)}{s^i} \sum_{j=0}^{3} d^{A,V}_{ij,f}\, \overline{\alpha}_s{}^j \ , \tag{4.3}$$

where $\overline{\alpha}_s = \frac{\alpha_s(\mu^2)}{\pi}$. For each quark not only the mass of the actual quark, but also the mass the b- and c-quark masses intervene in the radiator functions, each with different coefficients. In the $\overline{\text{MS}}$ scheme the expansion of the scale evolution of powers of the running masses reads as

$$m_q^2(s) = m_q^2(\mu)\Bigg(1 + 2\gamma_0 L \overline{\alpha}_s + \left(\gamma_0\beta_0 L^2 + 2\gamma_1 L + 2\gamma_0^2 L^2\right)\overline{\alpha}_s{}^2 \tag{4.4}$$

$$+\left[\frac{2}{3}\gamma_0\beta_0^2L^3+\gamma_0\beta_0L^2+2\gamma_2L+2\gamma_0^2\beta_0L^3+4\gamma_0\gamma_1L^2+\frac{4}{3}\gamma_0^3L^3\right]{\overline{\alpha}_s}^3\Bigg)\ ,$$

$$m_q^4(s)\ =\ m_q^4(\mu)\Bigg(1+4\gamma_0L\overline{\alpha}_s+\left(2\gamma_0\beta_0L^2+4\gamma_1L+8\gamma_0^2L^2\right){\overline{\alpha}_s}^2\Bigg]\ , \tag{4.5}$$

$$m_q^6(s)\ =\ m_q^4(\mu)\left(1+6\gamma_0L\overline{\alpha}_s\right)\ , \tag{4.6}$$

with $L=\ln x_\mu^2$. The new coefficients $d_{i,j}^{A,V}$ are related to those of Eqs. 3.33 and 3.34 by the following formulae.

Massless terms:

$$d_{00,q}^V=1+\frac{3}{4}Q_q^2\frac{\alpha(s)}{\pi}\ ,\ d_{00,q}^A=d_{00,q}^V, \tag{4.7}$$

$$d_{10,q}^V=1-\frac{1}{4}Q_q^2\frac{\alpha(s)}{\pi}\ ,\ d_{10,q}^A=d_{10,q}^V, \tag{4.8}$$

$$d_{20,q}^V=C_{02}+C_2^t\left(\frac{s}{m_t^2}\right)\ ,\ d_{20,q}^A=C_{02}+\left(C_2^t-2I_q^{(3)}\mathcal{I}^{(2)}\right)\left(\frac{s}{m_t^2}\right), \tag{4.9}$$

$$d_{30,q}^V=C_{03}\ ,\ d_{30,q}^A=C_{03}-2I_q^{(3)}\mathcal{I}^{(2)}; \tag{4.10}$$

$$\tag{4.11}$$

Terms in m_q^2:

$$d_{02,q}^V=0\ ,\ d_{02,q}^A=C_{20}^A, \tag{4.12}$$

$$d_{12,q}^V=C_{21}^V\ ,\ d_{12,q}^A=C_{21}^A, \tag{4.13}$$

$$d_{22,q}^V=C_{22}^V\ ,\ d_{22,q}^A=C_{22}^A+6\left(3+\ln\frac{m_t^2}{s}\right)-10\frac{s}{m_t^2}\left(\frac{8}{81}+\frac{1}{54}\ln\frac{m_t^2}{s}\right), \tag{4.14}$$

$$d_{32,q}^V=C_{23}^V\ ,\ d_{32,q}^A=C_{23}^A, \tag{4.15}$$

$$d_{32,b}^V=d_{32,c}^V=C_{23}\ ,\ d_{32,b}^A=d_{32,c}^A=C_{23}; \tag{4.16}$$

$$\tag{4.17}$$

Terms in m_q^4:

$$d_{04,q}^V=0\ ,\ d_{04,q}^A=C_{40}^A, \tag{4.18}$$

$$d_{14,q}^V=C_{41}^V\ ,\ d_{14,q}^A=C_{41}^A, \tag{4.19}$$

$$d_{24,q}^V=C_{42}^V+C_{42}^{V,L}\ln\frac{m_q^2(s)}{s}\ ,\ d_{24,q}^A=C_{42}^A+C_{42}^{A,L}\ln\frac{m_q^2(s)}{s}, \tag{4.20}$$

$$d_{24,b}^V=d_{24,b}^A=C_{42}-\ln\frac{m_b^2(s)}{s}\ ,\ d_{24,c}^V=d_{24,c}^A=C_{42}-\ln\frac{m_c^2(s)}{s} \tag{4.21}$$

$$d_{24,\hat{q}}^V=d_{24,\hat{q}}^A=12; \tag{4.22}$$

$$\tag{4.23}$$

Terms in m_q^6:

$$d_{06,q}^V=8\ ,\ d_{06,q}^A=0, \tag{4.24}$$

$$d^V_{16,q} = \frac{16}{27}\left(155 + 6\ln\ln\frac{m_q^2(s)}{s}\right),\ d^A_{16,q} = 0. \tag{4.25}$$

$$\tag{4.26}$$

Finally, to get the renormalisation scale dependence of the radiator functions, the terms of the type $m_q^j(s)\sum_i d_{ij}\alpha_s^i(s)/\pi$ in Eq. 4.3, dropping for clarity the axial-vector/vector and flavour indices, have to be replaced by the following expressions:

$$\sum_{j=0}^{3} d_{0j}\frac{\alpha_s^j(s)}{\pi} \to d_{00} + d_{10}\overline{\alpha}_s + (d_{20} + d_{10}\beta_0 L)\,\overline{\alpha}_s{}^2 \tag{4.27}$$
$$+ \left(d_{30} + (d_{10}\beta_1 + 2d_{20}\beta_0) + d_{10}\beta_0^2 L^2\right)\overline{\alpha}_s{}^3,$$

$$m_q^2(s)\sum_{j=0}^{3} d_{j2}\frac{\alpha_s^j(s)}{\pi} \to m_q^2(\mu)\Bigg[d_{02} + (d_{12} + 2d_{02}\gamma_0 L)\,\overline{\alpha}_s \tag{4.28}$$
$$+ \left(d_{12}\beta_0 L + d_{22} + 2d_{12}\gamma_0 L + d_{02}\gamma_0\beta_0 L^2 + 2d_{02}\gamma_1 L + 2d_{02}\gamma_0^2 L^2\right)\overline{\alpha}_s{}^2$$
$$+ \Bigg(d_{12}\beta_0^2 L^2 + d_{12}\beta_1 L + d_{32} + 2d_{22}\beta_0 L + \frac{2}{3}d_{02}\gamma_0\beta_0^2 L^3 + d_{02}\gamma_0\beta_1 L^2$$
$$+2d_{02}\gamma_1\beta_0 L^2 + 2d_{02}\gamma_2 L + 2d_{02}\gamma_0^2\beta_0 L^3 + 4d_{02}\gamma_0\gamma_1 L^2 + \frac{4}{3}d_{02}\gamma_0^3 L^3$$
$$+3d_{12}\gamma_0\beta_0 L^2 + 2d_{22}\gamma_0 L + 2d_{12}\gamma_1 L + 2d_{12}\gamma_0^2 L^2\Bigg)\overline{\alpha}_s{}^3\Bigg],$$

$$m_q^4(s)\sum_{j=0}^{2} d_{j4}\frac{\alpha_s^j(s)}{\pi} \to m_q^4(\mu)\Bigg[d_{04} + (d_{14} + 4d_{04}\gamma_0 L)\,\overline{\alpha}_s \tag{4.29}$$
$$\left(d_{14}\beta_0 L + d_{24} + 2d_{04}\gamma_0\beta_0 L^2 + 4d_{04}\gamma_1 L + 8d_{04}\gamma_0^2 L^2 + 4d_{14}\gamma_0 L\right)\overline{\alpha}_s{}^2\Bigg]$$

$$m_q^6(s)\sum_{j=0}^{1} d_{j6}\frac{\alpha_s^j(s)}{\pi} \to m_q^6(\mu)\Big[d_{06} + (d_{16} + 6d_{06}\gamma_0 L)\,\overline{\alpha}_s\Big] \tag{4.30}$$

The dependence of the radiator functions on the logarithm of the renormalisation scale $\ln x_\mu$ for a fixed input value of $\alpha_s(M_Z)$ is shown for each quark flavour in Fig. 4.

The shape of the scale dependence of R_V^q is almost identical for all flavours, except a small quark mass modification for the b-quark. A maximum in R_V^q appears around $\ln x_\mu = 0.5$ and a minimum at -1.75, spanning a difference of one per mil. The overall scale dependence of the axial-vector component R_A^q is twice as large as the one of R_V^q. As already observed for the dependence on α_s in Fig. 3, the shape of R_A^q is clearly different for up- and down-type quarks. For up-type quarks R_A^q becomes maximal at $\ln x_\mu = -0.3$, the maximum is close to the nominal value at $\ln x_\mu = 0$. The shape of the scale dependence is opposite for down-type quarks: a minimum appears at $\ln x_\mu = -1.1$. Considering the range of variation for x_μ from 1/2 to 2, corresponding to a range for $\ln x_\mu$ from -0.7 to 0.7, it appears that largest deviation from the nominal point at $\ln x_\mu = 0$ is not always obtained at the endpoints, but sometimes at smaller variations. Therefore, when assessing

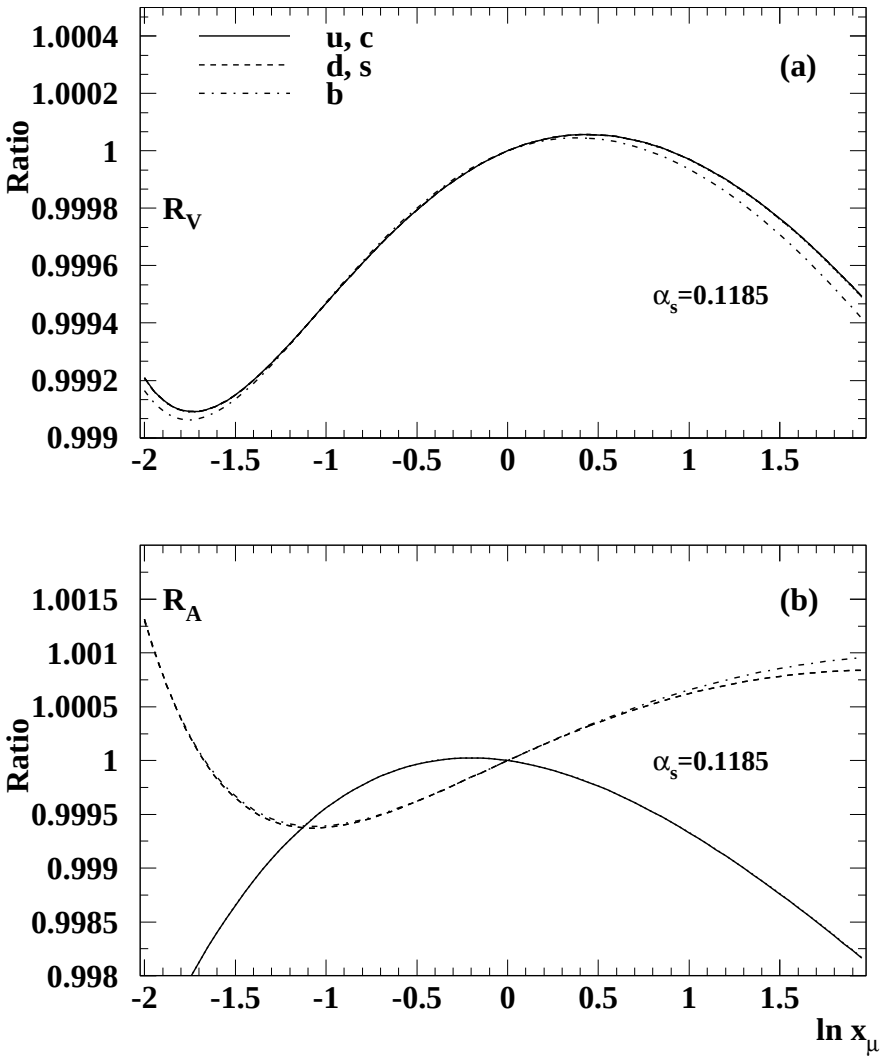

Figure 4: Dependence of the radiator functions on the renormalisation scale. The vector correction R_V^q (a) and the axial vector correction R_A^q (b) are shown for the quarks $q = u, d, s, c, b$ as function of $\ln x_\mu$, normalised to their value at $x_\mu = 1$.

the uncertainty for the observables studied in the following, the endpoints of $\ln x_\mu$ ($\ln x_\mu^-$ and $\ln x_\mu^+$) have been chosen to correspond to the largest change in the observables, within the pre-defined range $|\ln x_\mu| < 0.7$.

The dependence of the effective couplings on $\ln x_\mu$ is shown in Fig. 5. The quantities $|\rho_Z^f|$ and $|g_Z^f|^2$, as they appear in the expressions for the widths, are shown as ratio for ρ_Z^f but as shift for g_Z^f, i.e. $|g_Z^f|^2(\ln x_\mu) - |g_Z^f|^2(\ln x_\mu = 0)$. The shape of the couplings scale dependence is rather different from the radiator functions dependence and less structured, given by the interference of complete two-loop and incomplete leading three-loop corrections

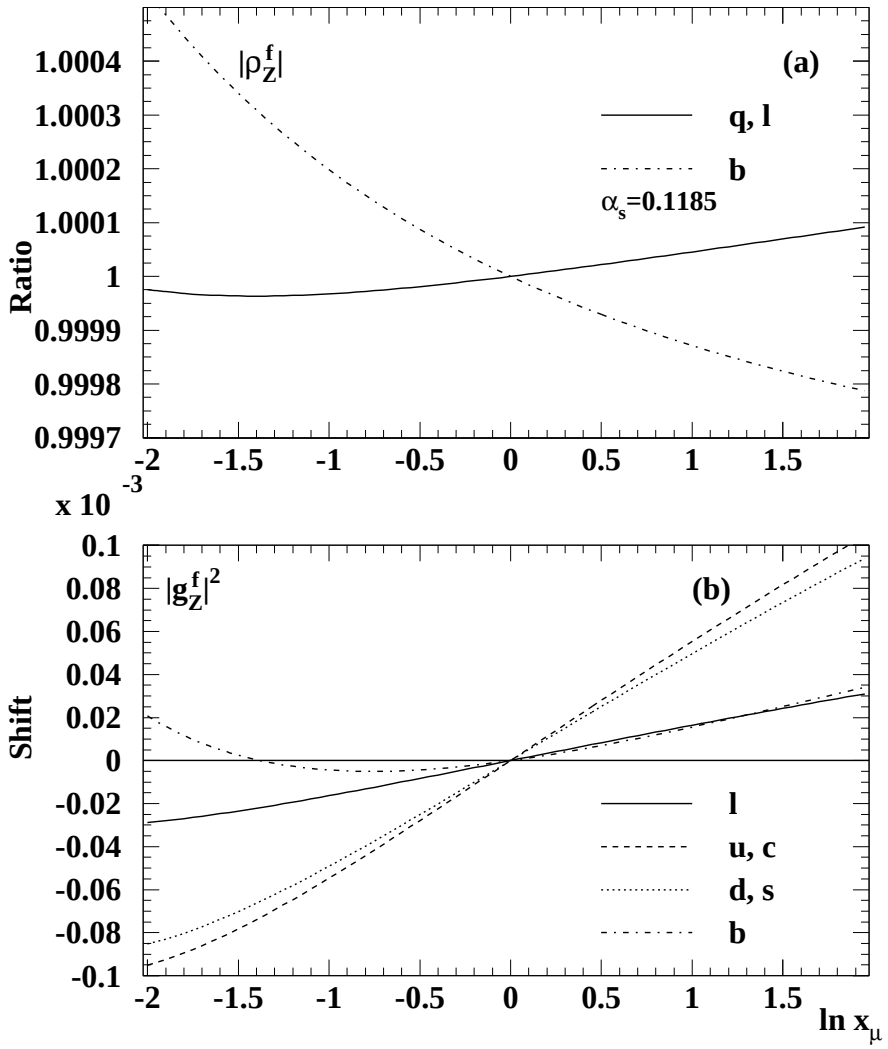

Figure 5: Dependence of the effective couplings $|\rho_Z^f|$ (a) and $|g_Z^f|^2$ (b) on the renormalisation scale.

to the mixed corrections. For all light quarks and leptons the relative change of $|\rho_Z^f|$ is only about 10^{-4}, for the b-quark much larger and amounts to 0.8 per mil. The absolute change of $|g_Z^f|^2$ is about $2 \cdot 10^{-4}$ for light quarks and $0.6 \cdot 10^{-4}$ for leptons and slightly less for b-quarks, corresponding to a relative change of less than two per mil for all quarks but almost one percent for the leptons.

Turning to the widths, for hadronic final states both the effective couplings and the radiator functions discussed above contribute to scale dependence. For the leptonic widths only the effective couplings depend on the renormalisation scale through the mixed corrections. The relative magnitude of contributions is given by the formulae for the widths, Eq. 3.1 for the leptons and Eq. 3.2 for the quarks. The scale dependence of the widths and

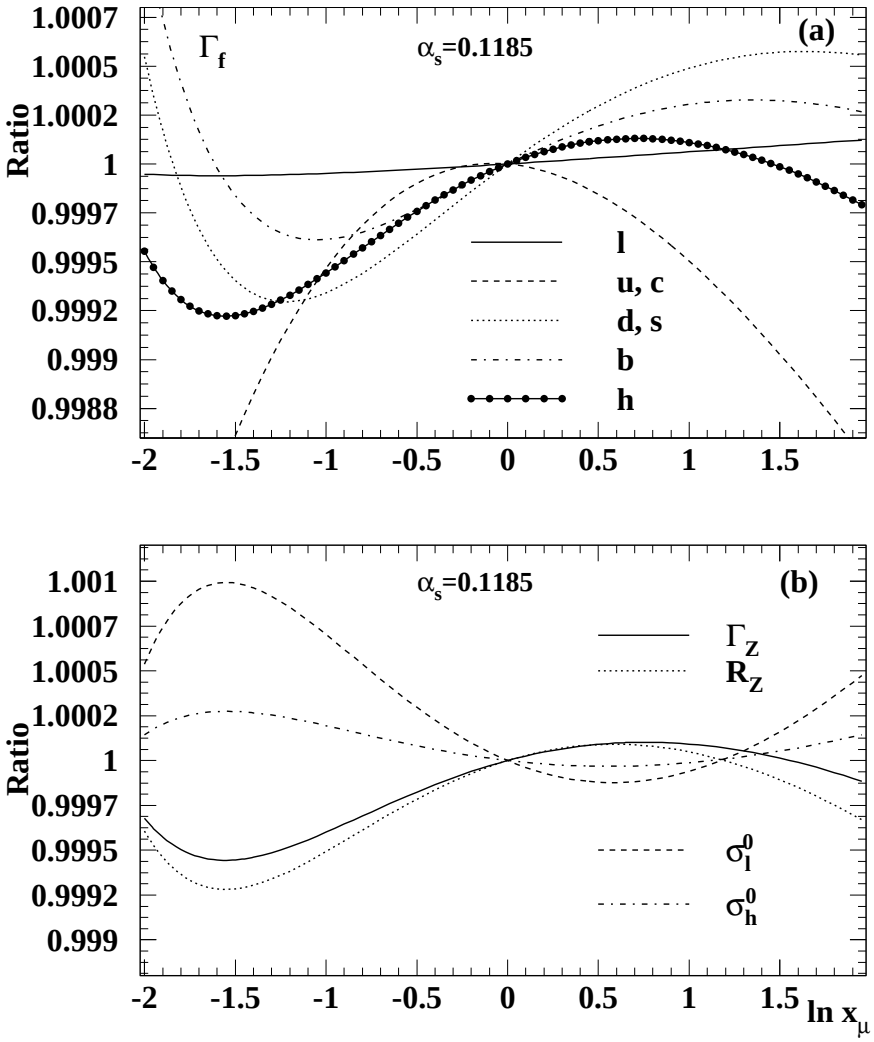

Figure 6: Dependence of the widths (a) and selected realistic observables (b) on the renormalisation scale for $\alpha_s(M_{\mathrm{Z}}) = 0.1185$.

of the realistic observables are shown in Fig. 6.

The shape of the scale dependence for the widths depends on the fermion type. For the u- and c-quark a maximum is found close to $\ln x_\mu = 0$, and variations of $\ln x_\mu$ in any direction entail a decrease of the width. The partial widths into d- and s-quarks increase monotonically from $\ln x_\mu = -0.7$ to $\ln x_\mu = 0.7$, similarly for the width of the b-quark, albeit with a flatter shape. The total hadronic widths of the Z boson emerges as sum of the quarkonic contributions, leading to an average shape of its scale dependence with a minimum at -1.6, a maximum at 0.7 with a difference of one per mil between them.

The scale dependence of the leptonic widths is clearly much weaker than that of the

quarkonic counterparts. In the central range of $\ln x_\mu$ the leptonic width changes by about a tenth of the hadronic width's change. The sensitivity of Γ_l to the renormalisation scale arise through the EW×QCD corrections, essentially those incorporated in ρ_Z^l.

4.2 Perturbative uncertainties for observables

The perturbative uncertainty for widths and realistic observables are defined as the difference between the observables value at $x_\mu = 1$ and at $x_\mu^{+/-}$, for a given input value of $\alpha_s(M_Z)$. The range of variation for x_μ, defined by x_μ^+ and x_μ^-, is chosen to generate the maximum and minimum values of the observables within the pre-defined range $1/2 \leq x_\mu \leq 2$. The absolute size of the perturbative uncertainty depends on the input value of α_s, for an observable calculated at NNLO its uncertainty is scaling with α_s^4. The relative systematic uncertainty for the widths and observables is shown in Fig. 7 as function of $\alpha_s(M_Z)$. Here and in Table 2 the relative uncertainties for a generic observable O are defined by

$$\Delta O = \frac{\left[O(x_\mu^\pm) - O(x_\mu = 1)\right]}{O(x_\mu = 1)} \,. \tag{4.31}$$

The positive and negative systematic uncertainties are generally asymmetric, for the widths of the u- and c-quark only the negative uncertainty contributes, given the particular shape of their scale dependence. The uncertainty for the width of down-type quarks is typically $\pm 0.05\%$, for up-type quarks it is -0.03% and for the leptonic width a factor of 10 smaller $\pm 0.005\%$. Among the realistic observables σ_l^0 has the largest uncertainty of about $+0.05\%$, the other variables uncertainty is about half that size.

For selected values of $\alpha_s(M_Z)$ the uncertainties for the observables are given in Table 2, where the scale variation endpoints $x_\mu^\pm$ are listed in the last column.

4.3 Contributions to the scale dependence

The three classes of higher order corrections analysed in Section 3.4 contribute to the perturbative uncertainty of the observables via their different evolution under the renormalisation scale variation. The size of the NNLO, quark mass and mixed EW⊗QCD corrections, given in Table 1, are typically at the level of one per mil, while the perturbative uncertainties are about 0.1 per mil (see Table 2). The absolute size of the corrections alone is not a reliable indicative of their contribution to the uncertainty, which must be evaluated from their scale dependence.

The scale uncertainty is therfore re-calculated without the NNLO contribution (i.e. dropping terms in $\mathcal{O}(\alpha_s^3)$ in Eqs. 3.33, 3.34), in which case also the evolution of $\alpha_s(\mu)$ in Eq. 3.71 has to be performed at NLO.

The contribution from the quark mass corrections is estimated by switching off the explicit scale dependence of the running quark masses (i.e. setting $m_q^p(s) = m_q^p(\mu)$ in Eqs. 4.5 - 4.6).

The impact of scale dependence of the mixed EW⊗QCD corrections is tested by eliminating the terms in the $\mathcal{O}(\alpha\alpha_s^2)$ corrections depending explicitly on x_μ.

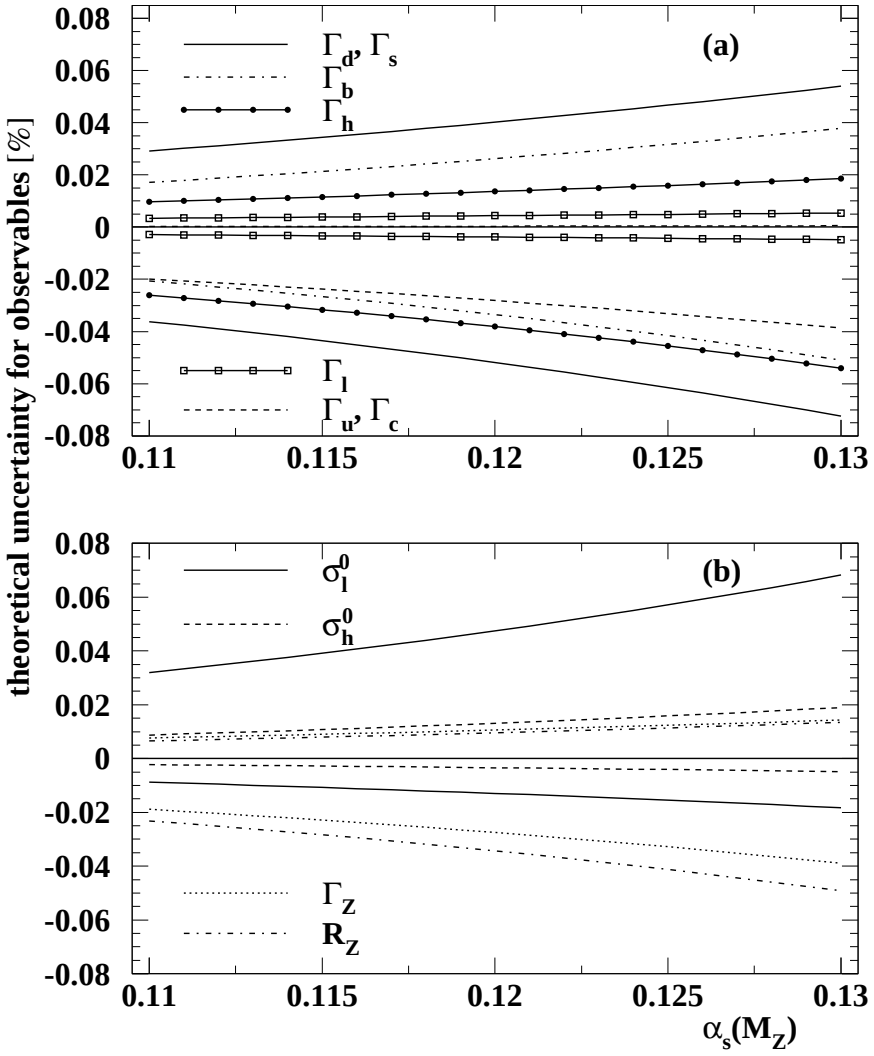

Figure 7: Relative perturbative uncertainty in percent for the widths (a) and selected realistic observables (b) as a function of $\alpha_s(M_Z)$.

The scale dependence obtained under these conditions is compared to the nominal scale dependence of the complete NNLO prediction in Fig. 8, considering as example Γ_Z and σ_h^0.

The change from NNLO to NLO entails a strongly increased scale dependence for the quarkonic widths, but with opposite effect on up- and down-type quarks, resulting in a weaker enhancement for the realistic observables. The uncertainties for the observables obtained as before by a scale variation between x_μ^+ and x_μ^- are summarised in Table 3 for the theories with modified scale dependence of higher order corrections. For the realistic observables the downgrade from NNLO to NLO results in an increase by a factor of two of

$\alpha_s(M_Z)$	0.110	0.115	0.120	0.125	0.130	$x_\mu^\pm$
Γ_u	0.002	0.003	0.003	0.004	0.006	0.925
	-0.199	-0.238	-0.282	-0.331	-0.387	2.0
$\Gamma_{d,s}$	0.292	0.344	0.403	0.468	0.540	2.0
	$-.363$	$-.435$	$-.519$	$-.615$	$-.725$	0.5
Γ_c	0.002	0.003	0.003	0.004	0.006	0.925
	$-.198$	$-.237$	$-.281$	$-.331$	$-.387$	2.0
Γ_b	0.172	0.214	0.262	0.317	0.379	2.0
	$-.207$	$-.266$	$-.335$	$-.416$	$-.510$	0.5
Γ_h	0.098	0.116	0.137	0.160	0.186	2.0
	$-.261$	$-.317$	$-.381$	$-.455$	$-.540$	0.5
Γ_l	0.035	0.039	0.044	0.049	0.054	2.0
	$-.029$	$-.033$	$-.038$	$-.043$	$-.048$	0.5
Γ_Z	0.076	0.090	0.106	0.124	0.143	2.0
	$-.189$	$-.229$	$-.275$	$-.328$	$-.389$	0.5
σ_h^0	0.088	0.108	0.131	0.158	0.190	0.5
	$-.023$	$-.028$	$-.034$	$-.041$	$-.049$	1.75
σ_l^0	0.320	0.391	0.475	0.571	0.682	0.5
	$-.088$	$-.107$	$-.130$	$-.155$	$-.183$	1.8
R_Z	0.066	0.080	0.096	0.114	0.135	1.8
	$-.232$	$-.284$	$-.343$	$-.413$	$-.492$	0.5

Table 2: Systematic perturbative uncertainties in per mil of EW observables for different values of $\alpha_s(M_Z)$. The last colum indicates the values of the renormalisation scale $x_\mu^\pm$ corresponding to the maximum variation of the observables with respect to their nominal values at $x_\mu = 1$, within the pre-defined variation range $1/2 \leq x_\mu \leq 2$

the perturbative uncertainty and the asymmetry between positive and negative uncertainty is also enlarged. For realistic observables the shape of the scale dependence without the running masses is similar but steeper than in the NNLO case. It has a large impact only for the b-quark, where the uncertainty is increased by a factor of three, which propagates to an increase of about 50% for the realistic observables.

The effect of dropping the scale dependence of the mixed corrections has in contrast to the other variations a net impact on the leptonic width, since this is the only source of sensitivity to QCD effects. The perturbative uncertainty for Γ_l is increased by a factor of three, the quarkonic width uncertainty by about 30-40 %. The realistic observables of ratios of widths are less sensitive to the mixed corrections and a moderate enhancement of the uncertainty of a few percent is observed, while for Γ_Z the effect from quarkonic and leptonic widths adds up to an almost doubled uncertainty.

In conclusion the stability of the predictions under scale variations depends crucially on the NNLO corrections, but depending on the observable also quark mass and to lesser extent mixed corrections contribute significantly to the accuracy of the calculations.

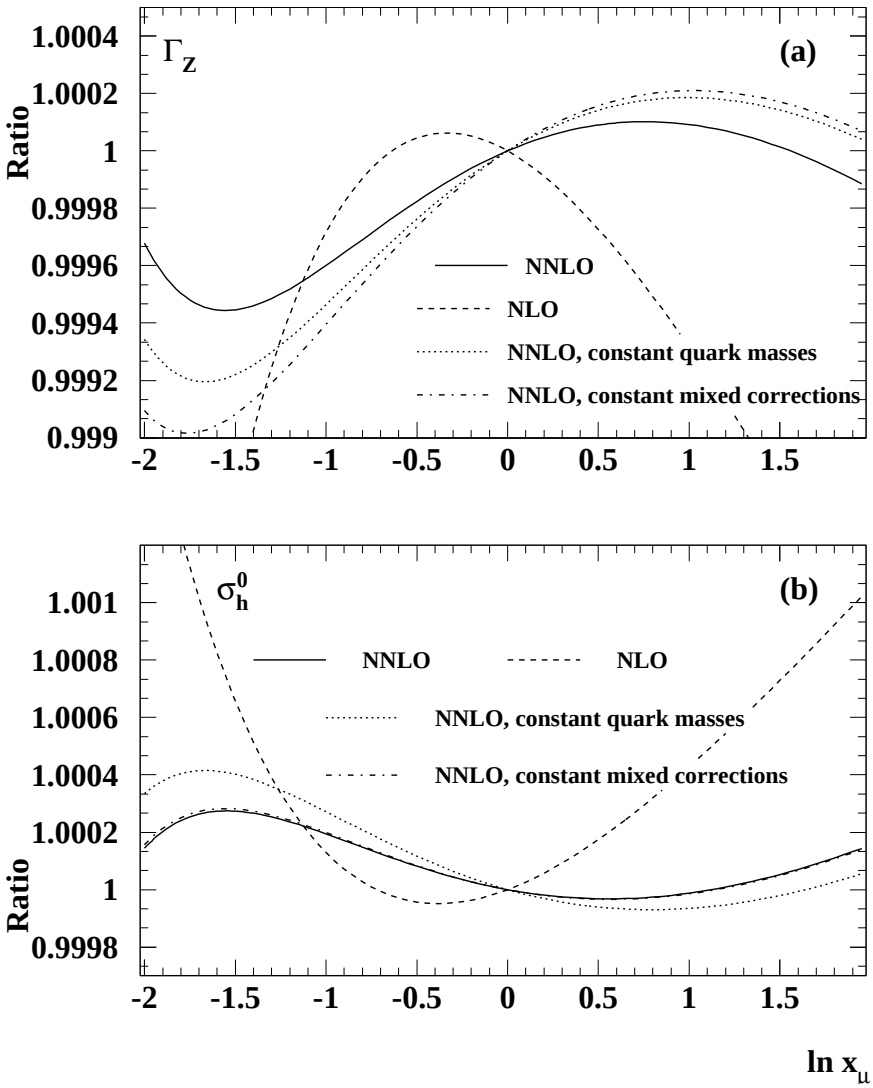

Figure 8: Renormalisation scale dependence of Γ_Z (a) and σ_h^0 (b) using the full NNLO prediction compared to reduced theories at NLO only, neglecting the scale dependence of the running quark masses and of the mixed EW⊗QCD corrections, for $\alpha_s(M_Z) = 0.1185$.

5. Perturbative uncertainties for α_s

In the context of global analyses of world electroweak data [1] $\alpha_s(M_Z)$ is fit together with four other free parameters of the standard model: M_H, M_Z, m_t and $\Delta\alpha^{(5)}_{had}$. The correlation between α_s and the other parameters is small. The observables included in the fit with a sizeable sensitivity to α_s are R_Z, Γ_Z and σ_h^0. The information from the leptonic pole cross section σ_l^0 is included in the other observables. This particular selection of observables is the result of an optimisation for the best accuracy for the five free SM parameters, which

Theory	NNLO	NLO	fixed quark mass corrections	fixed mixed corrections
Γ_u	0.003	1.430	0.003	0.004
	−0.268	−1.673	−0.268	−0.374
$\Gamma_{d,s}$	0.384	0.067	0.384	0.477
	−0.493	−0.851	−0.493	−0.628
Γ_c	0.003	1.431	0.004	0.004
	−0.268	−1.671	−0.291	−0.374
Γ_b	0.247	0.0230	0.684	0.339
	−0.313	−0.673	−0.879	−0.448
Γ_h	0.130	0.096	0.228	0.226
	−0.361	−0.615	−0.488	−0.502
Γ_l	0.042	0.042	0.042	0.121
	−0.036	−0.036	−0.036	−0.151
Γ_Z	0.101	0.063	0.170	0.189
	−0.260	−0.419	−0.349	−0.390
σ_h^0	0.124	0.265	0.174	0.126
	−0.032	−0.048	−0.069	−0.033
σ_l^0	0.448	0.923	0.626	0.477
	−0.122	−0.164	−0.255	−0.140
R_Z	0.091	0.115	0.186	0.106
	−0.325	−0.657	−0.452	−0.350

Table 3: Perturbative uncertainties (in per mil) for selected observables obtained from renormalisation scale variation at $\alpha_s(M_Z) = 0.1185$. The nominal NNLO uncertainty is compared to reduced theories where the scale dependence for certain classes of corrections is switched off.

may not necessarily be the optimal for α_s alone when the other parameters are fixed to their SM values. For example σ_l^0 has actually the best sensitivity through the inverse squared radiator functions and may be used alone to determine α_s from a single parameter fit, avoiding thereby the otherwise required correlations between the observables, and the dependence of α_s on the Higgs or top mass may be investigated.

Having in mind this scenario, the procedure is to determine in a first step the perturbative uncertainty for measurements of α_s using single selected observables and to estimate in a second step the uncertainty for a global fit including several variables.

The basic principle for the uncertainty estimation was developed in [2]: the systematic uncertainty for a given observable and fixed value of $\alpha_s(M_Z)$ (i.e. as obtained from a fit to this observable) is evaluated in the theory by variation of the renormalisation scale $x_\mu^- < x_\mu < x_\mu^+$. The change of the observables under the scale variation can also be generated by a variation of the input value of α_s at fixed $x_\mu = 1$. This procedure leads in general to two alternative values of α_s corresponding to the changes of the observable for x_μ^- and x_μ^+. The difference between the nominal value of α_s and these two alternatives finally determine the perturbative uncertainty of α_s.

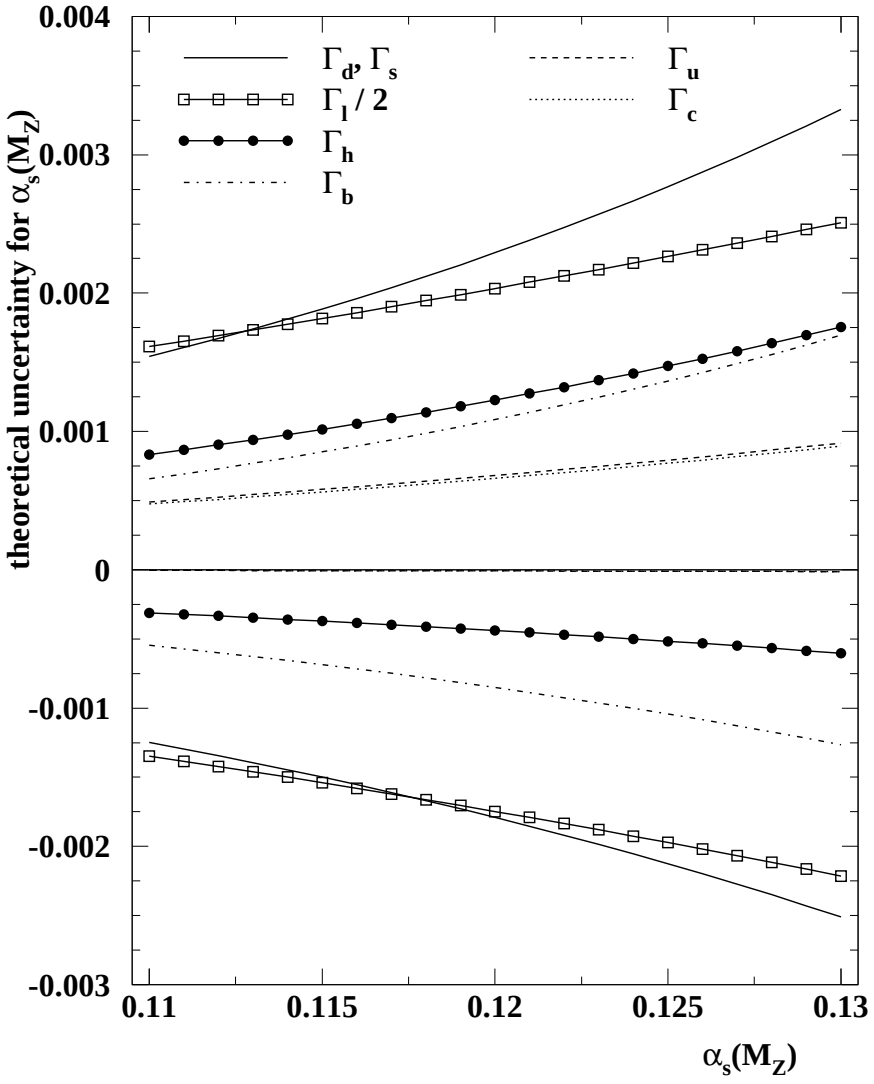

Figure 9: Positive and negative contributions to the perturbative systematic uncertainty of $\alpha_s(M_Z)$ determined from various partial widths of the Z boson. The uncertainty using Γ_l obtained at NLO is divided for representation by a factor of two.

The uncertainty itself depends on the type of observable and on the input value of α_s. At NNLO the size of the perturbative uncertainty scales as α_s^4. It is instructive to consider the uncertainty for α_s for the pseudo-observable widths in a first step, in order to understand their contribution to realistic observables. The systematic uncertainties are shown in Fig. 9 as function of the input value of α_s in a relevant range from 0.11 to 0.13.

As expected from the scale uncertainty of the width itself, there are large differences between the uncertainties of α_s determined using the widths of up-, down-type quarks and leptons. The size of the uncertainty for α_s is between one and two percent for quarks and

about 4 percent for leptons, QCD corrections for the leptonic widths being calculated only at NLO. Given the shape of the scale uncertainty for the width of the u- and c-quark, the resulting uncertainty of α_s is essentially one-sided. Also for the other widths a certain asymmetry in the uncertainty is observed, the positive (upward) uncertainty is generally larger than the negative (downward). This asymmetry may well be a technical artefact of the scale variation prescription, and conservatively the maximum of the positive and negative uncertainty is assigned as a symmetric uncertainty. For selected input values of $\alpha_s(M_Z)$ the symmetrised uncertainties are given in Table 4. The uncertainty of α_s determined from

$\alpha_s(M_Z)$	0.110	0.115	0.120	0.125	0.130
Γ_u	0.00049	0.00058	0.00068	0.00079	0.00092
$\Gamma_{d,s}$	0.00154	0.00189	0.00229	0.00277	0.00333
Γ_c	0.00047	0.00056	0.00066	0.00077	0.00089
Γ_b	0.00066	0.00085	0.00109	0.00136	0.00170
Γ_h	0.00083	0.00102	0.00123	0.00147	0.00176
Γ_l	0.00323	0.00363	0.00407	0.00453	0.00502

Table 4: Systematic perturbative uncertainties for measurements of α_s from EW observables. The symmetric uncertainty is given by the maximum of upward and downward uncertainties obtained by a renormalisation scale variation.

realistic electroweak observables is shown in Fig. 10. The perturbative uncertainty ranges between 1.3% for Γ_Z and 1.0% for σ_h^0. The largest uncertainty is observed in the case of Γ_Z, which is directly proportional to the product of effective couplings and radiator functions. The uncertainties from the other variables are very similar, between 1.0% and 1.1%. In R_Z the widths appear linearly in nominator and denominator, in σ_l^0 and σ_h^0 quadratic combinations of leptonic, hadronic and total widths of the Z boson interplay. As a consequence the scale dependence of the effective couplings and/or the radiator functions cancel to some extent in the ratio.

Several observables are included in the global EW fits [1], but only R_Z, Γ_Z and σ_h^0 have a sizeable sensitivity to α_s. Effectively, these three observables determine α_s and the perturbative uncertainty of α_s is bound to be an average of their individual contributions. The exact weights of each variable to the determination of α_s and subsequently to its perturbative uncertainties can not be determined in the framework of the present work. In order to derive nonetheless an estimate of the perturbative uncertainty from a global fit, a new variable

$$\Delta = \omega_1 \Gamma_Z + \omega_2 \sigma_h^0 + \omega_3 R_Z \ , \tag{5.1}$$

is introduced in order to approximate the sensitivity of the three real observables to α_s in a global fit by a single observable. The perturbative uncertainty for α_s obtained from the Δ variable is an indicative for the true uncertainty from a combined fit. The weights ω_i are determined from the sensitivity

$$\omega_i = \left| \frac{\partial O_i}{\partial \alpha_s} \right| \frac{\sigma(\alpha_s)}{\sigma(O_i^{exp})} \ , \tag{5.2}$$

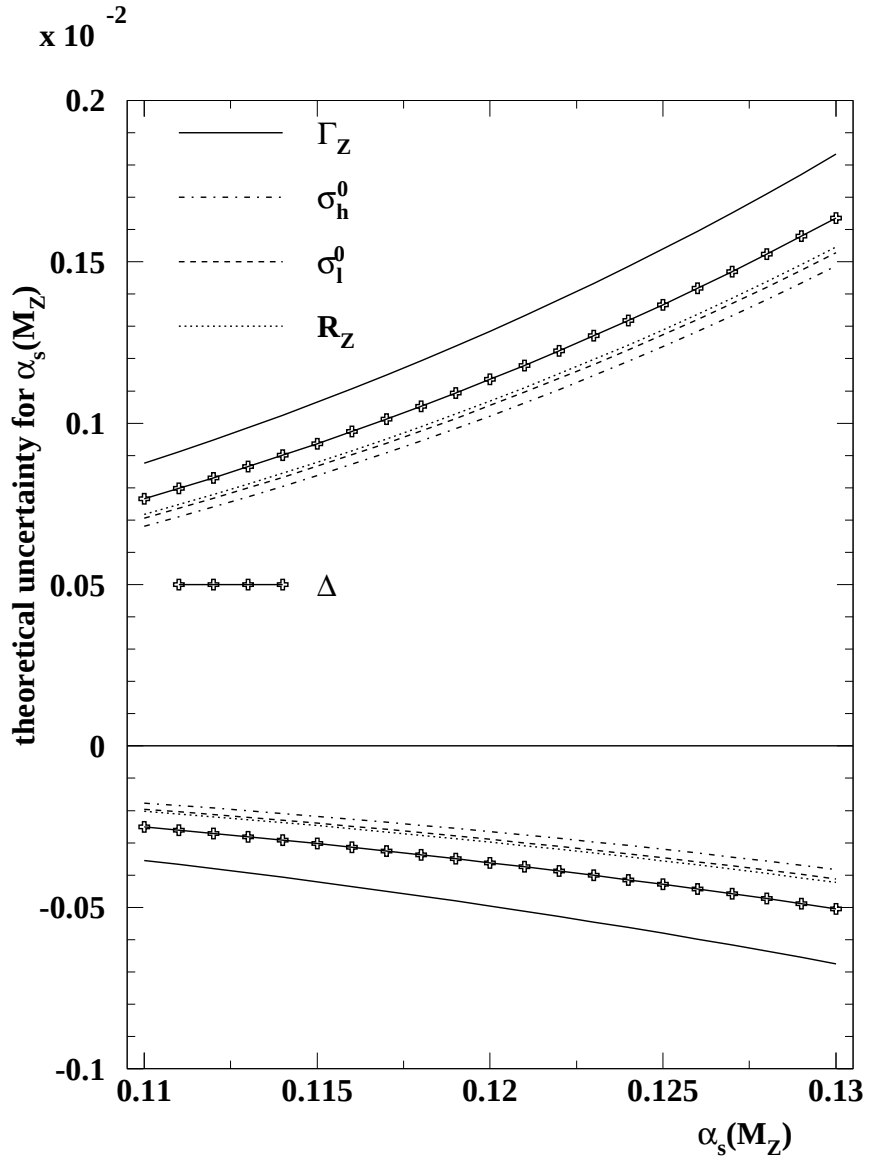

Figure 10: Systematic perturbative uncertainties for measurements of α_s using the EW observables Γ_Z, R_Z, σ_l^0 and σ_h^0 as function of the input value of $\alpha_s(M_Z)$. The quantity Δ denotes a weighted average of the uncertainty for Γ_Z, R_Z and σ_h^0, relevant for global analyses of electroweak data.

where O_i are the three observables, $\sigma(\alpha_s)$ is the uncertainty on α_s from the fit, taken to be 0.003 for all observables, and $\sigma(O_i^{exp})$ is the measured experimental uncertainty for the observables themselves. This procedure yields $\omega_1 = 0.36$, $\omega_2 = 0.23$ and $\omega_2 = 0.41$. The resulting uncertainty from Δ is also shown in Fig. 10. The upper and lower bounds of the combined uncertainty can be estimated assuming that the true weights of the observables in a global fit are all positive. In this case the combined uncertainty can not be larger or smaller than any of the individual contributions from the single observables.

In Table 5 the symmetric perturbative uncertainties are summarised for the realistic

observables and for the Δ variable in a narrow range around 0.119. The possible variations for the combined uncertainty are also given as Δ^+ for the upper and Δ^- for the lower bound. As a stability test, the weights in the calculation of Δ have been set constant for all observables. The resulting combined uncertainty does not change by more than 0.00001.

$\alpha_s(M_Z)$	0.118	0.119	0.120	0.121	0.122	a	b
Γ_Z	0.00119	0.00124	0.00128	0.00133	0.00138	$-1.22 \cdot 10^{-4}$	6.80
σ_h^0	0.00095	0.00098	0.00102	0.00106	0.00110	$-1.70 \cdot 10^{-4}$	5.77
σ_l^0	0.00098	0.00101	0.00105	0.00110	0.00114	$-1.60 \cdot 10^{-4}$	5.88
R_Z	0.00099	0.00103	0.00107	0.00111	0.00115	$-1.55 \cdot 10^{-4}$	5.92
Δ	0.00105	0.00109	0.00114	0.00118	0.00122	$-1.50 \cdot 10^{-4}$	6.22
Δ^+	0.00119	0.00124	0.00128	0.00133	0.00138		
Δ^-	0.00095	0.00098	0.00102	0.00106	0.00115		

Table 5: Systematic perturbative uncertainties for measurements of α_s from EW observables. The symmetric uncertainty is given by the maximum of upward and downward uncertainties obtained by a renormalisation scale variation. The variable Δ represents the combined uncertainty for a global fit including Γ_Z, σ_h^0 and σ_l^0, with upper bound Δ^+ and lower bound Δ^-.

For a value of $\alpha_s(M_Z) = 0.12$ the perturbative uncertainty ranges from ± 0.00102 for σ_h^0 to ± 0.00128 for Γ_Z, with a weighted average of ± 0.00115 (unweighted ± 0.00114).

The dependence of the symmetric uncertainty on the input value of $\alpha_s(M_Z)$ can smoothly be parameterised to form $a + b \cdot \alpha_s(M_Z)^4$. The parameterisation, valid for $0.11 \leq \alpha_s(M_Z) \leq 0.13$, allows for an interpolation of the uncertainty between calculated points. The parameters a and b are given for each observable in Table 5. The result of the parameterisation is compared in Fig.11 to the exact calculation, which is reproduced to good accuracy.

5.1 Experimental tests

In order to substantiate the uncertainty estimate, a fit is performed to a set of test data taken from the preliminary LEP combination [1]. In the fit to the test data, the value of α_s is determined for $x_\mu = 1$ (nominal case) and x_μ^+, x_μ^- for the uncertainty. Only realistic observables are considered and the other SM parameters are fixed to the values given in Section 2. The central values, experimental systematic uncertainties and correlations between the observables used are given in Table 6 (taken from [1]). A fit to the test

observable	central value	experimental uncertainty	correlations Γ_Z	σ_h^0	R_Z
Γ_Z[GeV]	2.4952	0.0043	1.0	-0.297	0.004
σ_h^0[nb]	41.540	0.037		1.0	0.183
R_Z	20.767	0.024			1.0
σ_l^0[nb]	2.0003	0.0027			

Table 6: Test data for the EW observables. The numerical values are preliminary results taken from [1], since σ_l^0 is not included in the global fit its correlation data is not available.

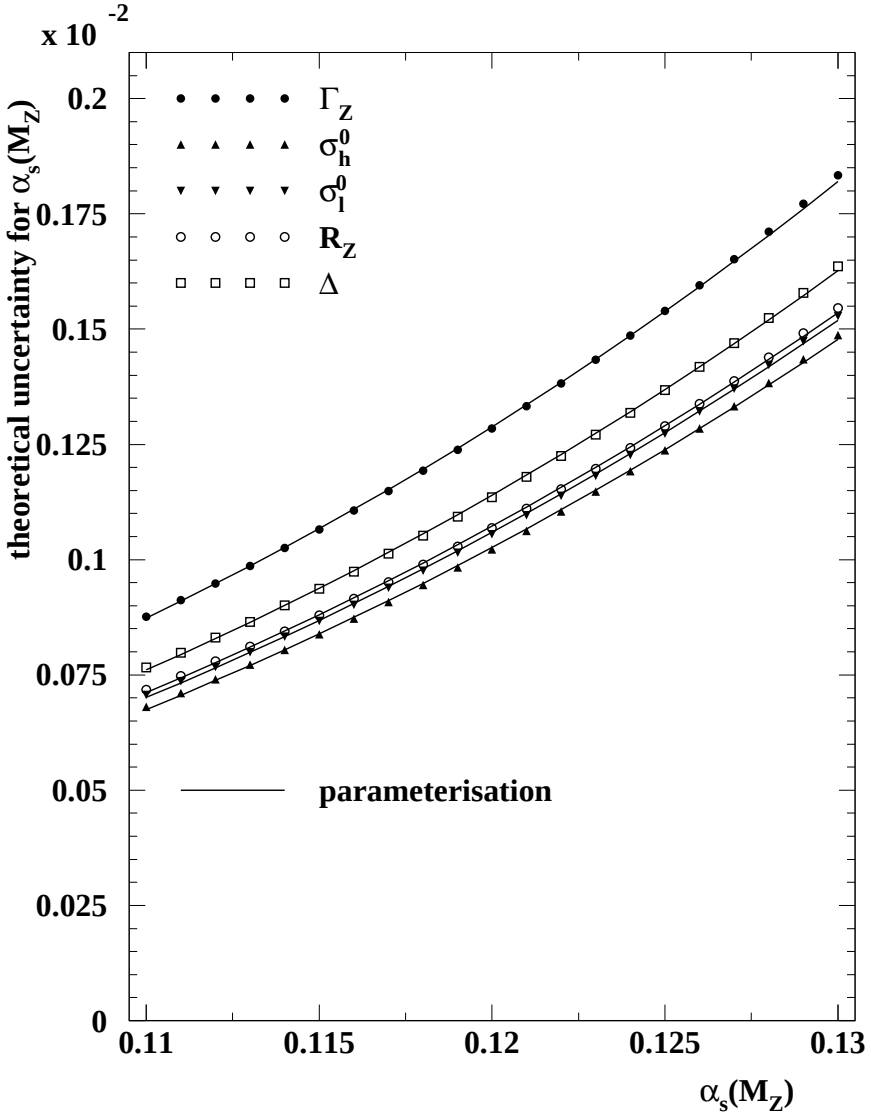

Figure 11: Symmetrised systematic perturbative uncertainties for measurements of α_s using the EW observables. The quantity Δ denotes an weighted average of the uncertainty for Γ_Z, R_Z and σ_h^0, relevant for global analyses of electroweak data. The symbols show the exact calculation and the lines represent the result of the parameterisation.

data yields results for α_s summarised in Table 7. The central values for fits using single observables are close to the world average [4] apart from σ_h^0 which yields a very low value of α_s with a large experimental uncertainty of 6%. As expected, the smallest error of 3% is obtained for σ_l^0 having the best sensitivity. The perturbative uncertainties obtained in this test are in good agreement with the data-independent method summarised in Table 5. The case of σ_h^0 yielding a small theoretical uncertainty originating from its small central result illustrates the bias appearing when the uncertainty is determined from an actual

measurement. This bias can be reduced by taking a combined world average for α_s in the theoretical estimation of the perturbative uncertainty.

The experimental precision of fits to several observables is increased to 3% for the canonical ensemble of Γ_Z, σ_h^0 and R_Z which is also used by the global EW fits [1]. The perturbative uncertainty is again consistent with the result obtained previously for the Δ variable. The observables σ_h^0 with less sensitivity may be exchanged by σ_l^0 in the data sample to be fit. The correlation of experimental uncertainties between σ_l^0 and the other variables is unknown, as a crude approximation the same correlation as for σ_h^0 is assumed. Under this reserve the experimental uncertainty is further reduced to 2% with essentially unchanged perturbative uncertainties. As the experimental uncertainty dominates the precision for α_s, the replacement of σ_h^0 by σ_l^0 might be considered for the global EW fits.

included observable	central value	experimental uncertainty	x_μ^+	x_μ^-	perturbative uncertainty
Γ_Z	0.1174	0.0041	0.1170	0.1186	$-0.00043 + 0.00122$
σ_h^0	0.1076	0.0065	0.1074	0.1082	$-0.00015 + 0.00063$
R_Z	0.1231	0.0037	0.1228	0.1244	$-0.00033 + 0.00125$
σ_l^0	0.1187	0.0030	0.1184	0.1197	$-0.00027 + 0.00104$
Γ_Z, σ_h^0, R_Z	0.1191	0.0027	0.1188	0.1203	$-0.00043 + 0.00113$
Γ_Z, σ_l^0, R_Z)*	0.1202	0.0021	0.1199	0.1213	$-0.00031 + 0.00114$

Table 7: Fit results for $\alpha_s(M_Z)$ from fits to various test data sets. The central result is obtained for $x_\mu = 1$, the perturbative uncertainty from a variation for the renormalisation scale from x_μ^+ to x_μ^-.)* In the combined fit to Γ_Z, σ_l^0 and R_Z the correlation for σ_l^0 is assumed to be the same as for σ_h^0.

The LEP electroweak working group has adopted another strategy to incorporate the QCD uncertainties in the global fits. From the perturbative uncertainties for the observables Γ_Z, σ_h^0 and R_Z themselves, given in Table 2, a covariance matrix was constructed and added to the other covariance matrices related to statistical and further systematic uncertainties. The total covariance matrix is then included in the global fit. While the central value of α_s does not change significantly when the QCD covariance matrix is added, its total uncertainty does increase and by quadratic subtraction of the non-QCD uncertainties a perturbative uncertainty of ± 0.0010 is obtained [23]. This result confirms the estimate of perturbative uncertainty based on theoretical considerations for the Δ variable given in Table 5.

6. Conclusions

A new method has been presented for the perturbative uncertainties at NNLO of measurements of α_s obtained from global analyses of precision electroweak data. The systematic uncertainties are obtained by a variation of the renormalisation scale in the calculations of final state QCD and mixed QCD⊗EW corrections for the electroweak observables included in the global analyses used to determine α_s and other Standard Model parameters. The

NNLO massless corrections, quark mass corrections and mixed QCD⊗EW corrections are observed to contribute to the theoretical predictions for the observables at the level of one per mil. Individual contributions to the renormalisation scale dependence have been studied in detail and the resulting uncertainty has been calculated for the widths of the Z boson into different quark flavours and leptons. For electroweak observables used to constrain the Standard Model and determine $\alpha_s(M_Z)$ the corresponding perturbative uncertainty for a value of $\alpha_s(M_Z) = 0.12$ is estimated to be between ± 0.0010 and ± 0.0013, in average ± 0.0011. The size of the perturbative uncertainty has been cross-checked with a toy fit to experimental test data. The determination of α_s at NNLO from electroweak data is one of most precise measurements of $\alpha_s(M_Z)$. Its precision is dominated by experimental effects yielding a relative uncertainty of about 3%, while perturbative uncertainties contribute only 1%.

Acknowledgements

The author would like to S. Bethke who has initially raised the issue of the perturbative uncertainties in this context. The author is indebted to G.P. Salam and R. Harlander for providing the essential ingredient on the renormalisation scale variation in presence of running quark masses. This article would not have been completed without the expertise provided by M. Grünewald on the topic of precision electroweak measurements and constraints on the Standard Model.

References

[1] The LEP Collaborations ALEPH, DELPHI, L3, OPAL, the LEP Electroweak working group, the SLD Electroweak and Heavy Flavour Working group, "*A Combination of preliminary Electroweak Measurements and constraints on the Standard Model*", hep-ex/0412015

[2] R. Jones, M. Ford, G.P. Salam, H. Stenzel and D. Wicke "*Theoretical uncertainties on α_s from event-shape variables in e^+e^- annihilations*", JHEP **12** (2003) 007.

[3] D.E. Soper and L.R. Surguladze, "*On the QCD perturbative expansion for* $e^+e^- \to$ *hadrons*", Phys. Rev. **D54** (1996) 4566.

[4] S. Bethke, Nucl. Phys. Proc. Suppl. **135** (2004) 345.

[5] S. Bethke, J. Phys. **G 26** (2000) R27.

[6] D. Bardin et al., "*ZFITTER v.6.21 - A Semi-Analytical Program for Fermion Pair Production in* e^+e^- *Annihilation*", Comput. Phys. Commun. **133** (2001) 229.

[7] A. Czarnecki and J. H. Kühn, Phys. Rev. Lett. **77** (1996) 3955.

[8] R. Harlander, T. Seidensticker, and M. Steinhauser, Phys. Lett. **B426** (1998) 125.

[9] M. Steinhauser, Phys. Lett. **B429** (1998) 158.

[10] H. Burkhardt and B. Pietrzyk, Phys. Lett. **B513** (2001) 46.

[11] B. A. Kniehl, Nucl. Phys. **B347** (1990) 86.

[12] M. Consoli, W. Hollik, and F. Jegerlehner, "*Electroweak radiative corrections for Z physics*", in *Proc. of Workshop on Z Physics at LEP, Geneva, Switzerland, Feb 20-21 and May 8-9, 1989,* report CERN 89–08 (1989)

[13] L. Avdeev, J. Fleischer, S. Mikhailov, and O. Tarasov, Phys. Lett. **B336** (1994) 560, E: ibid., **B 349** (1995) 597;
K. G. Chetyrkin, J. H. Kühn, and M. Steinhauser, Phys. Lett. **B351** (1995) 331.

[14] K. G. Chetyrkin, J. H. Kühn, and M. Steinhauser, Phys. Rev. Lett. **75**, (1995) 3394.

[15] A. Akhundov, D. Bardin, and T. Riemann, "*Electroweak one loop corrections to the decay of the neutral vector boson*", Nucl. Phys. **B276** (1986) 1.

[16] J. Fleischer, O. V. Tarasov, F. Jegerlehner, and P. Raczka, Phys. Lett. **B293** (1992) 437.

[17] J. Fleischer, O. V. Tarasov, and F. Jegerlehner, Phys. Lett. **B319** (1993) 249.

[18] K. G. Chetyrkin, A. L. Kataev, and F. V. Tkachev, Phys. Lett. **B85** (1979) 277.

[19] M. Dine and J. Sapirstein, Phys. Rev. Lett. **43** (1979) 668.

[20] W. Celmaster and R. J. Gonsalves, Phys. Rev. Lett. **44** (1980) 560.

[21] S. G. Gorishny, A. L. Kataev, and S. A. Larin, Phys. Lett. **B273** (1991) 141.

[22] K. Chetyrkin, J. Kühn, and A. Kwiatkowski, "QCD corrections to the e^+e^- cross-section and the Z boson decay rate", in *Reports of the Working Group on Precision Calculations for the Z Resonance,* report CERN 95–03 (1995) (D. Bardin, W. Hollik, and G. Passarino, eds.), pp. 175–263.

[23] M. Grünewald, private communication.